Response to comments on *Simplifying the calculation of light scattering properties for black carbon fractal aggregates*, ACPD **14**, 3537–3562, 2014.

A. J. A. Smith & R. G. Grainger

We are greatful for the submissions from referees and short commenters. All comments have been instructive and we feel have helped improve the structure and content of the paper. Responses will be made to each commenter in turn, starting with the referees. The original comments are provided in *italics* for reference. Modifications to the text have been highlighted.

Response to referee #1

1. One of the simplest and most popular algorithms for light scattering properties of the fractal aggregates is known as the Rayleigh-Debye-Gans (RDG) method, which has simple formulae and is highly efficient for calculations of any circumstance. Thus, before evaluating any parameterization on light scattering properties of the fractal aggregates, its accuracy compared with the direct approximations from the RDG should be checked. If the RDG can give similar accuracy, it becomes really meaningless to carry out any of those parameterizations. I think it is of great interest to add RDG results in the comparison, since RDG is a much more flexible and practical method.

As previously mentioned in Bond and Bergstrom (AST, 2006, §5.2 and references therein), the RDG method can under-predict absorption by 30 %. Using the descriptions from Sorensen (AST, 2001) with a structure factor parameterized as suggested by Lin et al. (Phy. Rev. A, 1990), this indeed seems to be the case. In Fig R1, we show the comparison of these RDG calculations and our parameterisaton to the MSTM calculations for scattering and absorption cross-sections. At longer wavelengths, differences between absorption in RDG and MSTM can be greater than 35 %. As such, we feel that the parameterisation presented in this paper is a useful improvement on RDG calculations. A brief summary of RDG has been added to Section 1.3, *Light scattering methods*, including discussion of the under-prediction of absorption. It reads: "An intermediate step between the rigour of MSTM and the simplicity of assuming spherical aerosols is Rayleigh-Debye-Gans theory (RDG) which assumes that the individual scattering spherules are small enough to be Rayleigh scatterers, and that these scatterers have a negligible multiple scattering interaction with each other. Further details can be found in the review paper by Sorensen (2001). However, as noted by Bond and Bergstrom (2006, §5.2 and references therein),

several studies have shown an underprediction of fractal aggregate absorption by RDG compared to rigourous light scattering calculations, particularly at longer wavelengths."

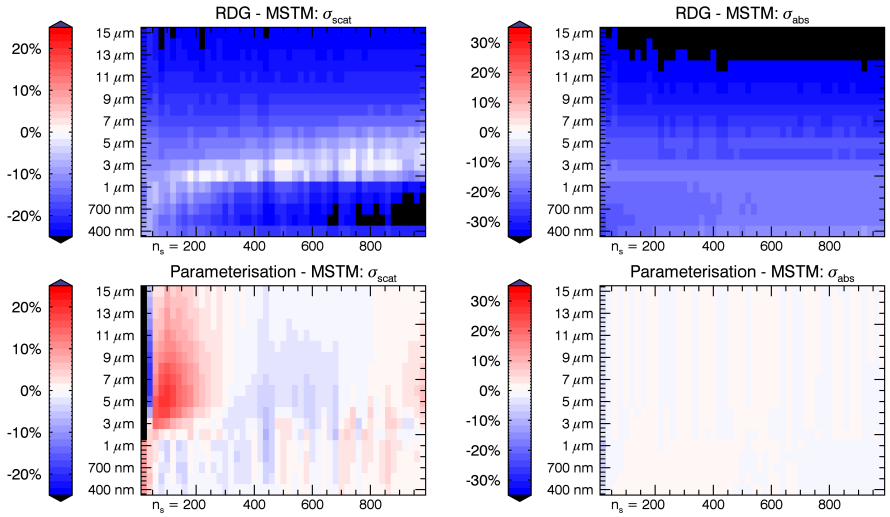

Figure R1: Differences in the scattering and absorption cross-sections of RDG and the parameterisation defined in the paper to MSTM calculations. The top row shows RDG relative differences to MSTM. The bottom row parameterisation differences.

2. Page 3540: The authors discuss the aging of BC as well as its effects. Yin and Liu (JQSRT 2010; 11: 2115-2126) and Liu et al. (AST 2012; 46: 31-43) built a simple model to study the scattering properties of coated aggregates, and can be easily adapted for this study (by also applying the effective medium approximations). From their work, the coating enhances not only the absorption but also the scattering of the aggregates, and their work should be mentioned.

A description of recent investigations of coating of BC has been added to the introduction at the end of section 1.1. This includes the suggested references, as well as discussion of the reduced absorption enhancement seen when aggregates are not fully embedded, as suggested by Referee #2. The additioal sentences read: "Once the BCFAs become hydrophilic, they can take on moisture and collapse into much more tightly packed "globules" (Mikhailov et al., 2006). These have greatly increased scattering and absorption cross-sections and greater forward scattering (Yin and Liu, 2010; Liu et al., 2012). Some recent discussions have focused on apparent discrepancy in absorption enhancement by the coating of BCFAs between measurement and models (Cappa et al., 2013). It has been noted that both the compactness and positioning of the BCFA within a coating medium have significant effects on mass absorbing cross-section (MAC) (Adachi et al., 2010; Scarnato et al., 2013)."

3. The right panel of Fig. 5: The asymmetry parameters for most aggregates shown in the figure are less than 0.4, whereas the color bar chosen can hardly show the details of their values.

Agreed. The colour bar has been adjusted.

4. Page 3544: The authors try to use the scattering properties of spheres to represent those of fractal aggregates, and it should be noticed: even appropriate spheres can be found for the cross sections and asymmetry parameters, the accuracy of such approximations is significantly challenged for the phase function, which was investigated in Li et al. (JQSRT 2010; 111: 2127–2132 that is cited in the manuscript).

Agreed. We had hoped that using a simpler property than the phase function, we might be more easily able to find a match, but this was not the case. A mention of this aspect of Li et al.'s work has been added at the end of section 3.2: "Earlier work by Li et al. (2010) had found that it was not possible to represent the phase function for a reasonable size distribution of BCFAs with a similar distribution of spheres at wavelengths of $\lambda = 0.628$ and $1.1\,\mu$m, so even had a good fit of σ_{ext}, σ_{sca}, and g been found, it is unlikely that the full phase function resulting would have been appropriate."

5. In Fig. 7, the authors show only the performance of the spherical approximation at wavelength of 550 nm, and demonstrate that the errors do not improve with increased wavelength. However, as the wavelength increases, the size parameter of the particle decreases, and the scattering properties should be simple and close to those of Rayleigh scattering. How do the errors distribute at large wavelengths (e.g. 12 μm), and are they still over 15% for most cases or just for few special n_s or D_f? A figure similar to Fig. 7 but for large wavelength will be interesting to discuss if the spherical approximation shows difference performance.

A very good point. At larger wavelengths, the fits are indeed better, but still not acceptable. Taking the case of 12 μm, the principal issue is that in the Rayleigh limit, the phase function is symmetric about scattering angles of $\pi/2$ forward and backwards scattering are equal, but this is not the case for the less compact aggregate particles. As such, one can either fit the extinction and scattering cross-sections but not the asymmetry, or vice-versa. This can be seen in the requested Fig. R2 where errors in scattering and extinction have been reduced to less than 5 % in almost all cases, but with resultant absolute errors in asymmetry of up to 0.2 for less compact BCFAs (with very large relative errors).

Discussion of this, and the figure have been added to the manuscript: "One might expect that at longer wavelengths as the scattering BCFAs approached the Rayleigh limit, the ability to fit spheres would improve. However, the asymmetry parameter at these wavelengths is non-negligible for the less compact and larger BCFAs (unlike Rayleigh scatterers) as can be seen in Figures 6 and 7. This means that it is not possible to find spheres that can match $\ln \sigma_{\text{ext}}$ and $\ln \sigma_{\text{sca}}$, whilst also having a large enough g. As such, a trade off between large errors in either the cross-sections, or asymmetry must be made. The fit with large errors in g is shown in Fig. 9."

6. Table 1 shows that coefficients 1 for SSA and g are both zero at 550 nm, and this indicates that it is not necessary to consider the linear term in Equations 3 and 4 for SSA and g. Is it true for all wavelengths or just for this single case, and this should be clarified in the paper.

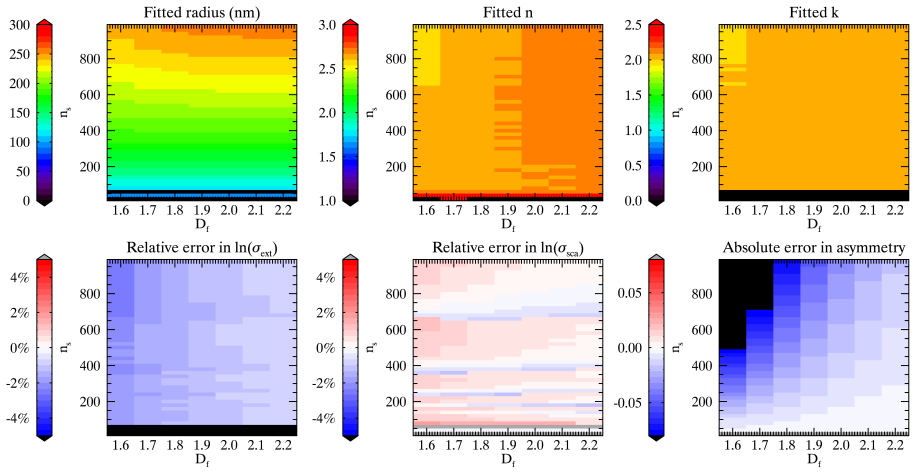

Figure R2: Fitted spheres for BCFA MSTM calculations with a wavelength of $\lambda = 12$ μm. In order to correctly characterise scattering and extinction, asymmetry errors had to be significantly increased. This figure has been added to the manuscript.

This is the case at shorter wavelengths only, as can be seen from inspecting the supplementary material. In general, for both SSA and g, at shorter wavelengths the linear coefficients are small, while at longer wavelengths, the logarithmic coefficents are small. A short discussion of this has been added to the caption for Table 1: "While the values of coefficient 1 (the linear term) in the fits of SSA and g are negligible at 550 nm, they increase at longer wavelengths while the values of coefficient 2 (the logarithmic term) decrease."

7. The bottom panels of Fig. 7 have some curves, which are not explained in the paper, and the numbers listed in Fig. 9 are not well discussed. All those should be detailed in the captions or the manuscript.

The curves in Fig. 7 marked the value (also represented by that data point's colour) at each data point in the image with a line at the extent of the box showing that the value was exactly equal to the maximum of the colour range for the plot. These were accidentally left in from a previous iteration of the plot (to check that the colours were correctly representing the values) and have now been removed. This definitely improves the clarity of the plot. Apologies.

The values in Fig. 9 are areas under the curves, and differences between areas. A description of their meanings has been added to the caption for Fig. 9. It reads: "The MSTM calculations (Data) are blue, the fitted data for the same radii (Fit) are orange, and the missing area covered by the fit, but not the MSTM calculations (Missing) are red. Numbers in these colours give the area under the respective curves. Δ gives the difference in areas between Data and Fit."

8. Page 3548/Conclusions: Although the spheres cannot be used to model the optical properties of fractal aggregates accurately, there are still other approximations that are efficient enough for GCMs (such as RDG mentioned above). Furthermore, considering the uncertainties on the parameters of the fractal ag-

gregates (e.g. k_f, D_f, and size distribution), the errors cased by the RDG or even the spherical approximations may be much smaller. Thus, the parameterization should not be the only way to consider the BC aerosol in GCMs.

Agreed. A comment following this gist has been added to the conclusions: "Other approximations such as RDG can improve greatly the representation of BCFA optical properties but generally do not provide sufficient absorption. With this in mind, a prudent step for GCMs requiring constantly changing distributions of BC aerosol could be to include a parameterisation such as this one which is computationally trivial to implement and is valid within the range of black carbon particles seen in the atmosphere. Uncertainties in the size distribution, shape, and composition of these particles should not be forgotten and will certainly cause differences at least as large as the simplification of optical properties to spheres or RDG."

Response to referee #2

1. There is a general inconsistency of how an aggregate of black carbon spheres is referred in the text (BC, BCFAs or soot).

Agreed. On inspection, all references to soot could be replaced with BC and this has been done.

2. In a subsection of the introduction, section 1.1, the authors present a physical description of aerosol formation and ageing. The authors mention the absorption enhancement due to coating and refer to few papers (Fuller 1999, Jacobson 2001, Bond 2006). Absorption properties of black carbon and appropriate parameterization are a major topic, due to climatological relevance and there could be cited more recent literature, i.e. Liu et al., 2012; Kahnert et al., 2012; Adachi et al., 2010. Also, it has been found both in field campaign and using numerical computations that, when black carbon aggregates are not fully embedded in the transparent coating there is no or little absorption enhancement, please add in the text, as well, Cappa et al, (2012, 2013) and Scarnato et al., (2013), as references.

Based on this and the comments by reviewer #1, the description of aggregate coating has been extended to include these points, at the end of section 1.1. It now reads: "Once the BCFAs become hydrophilic, they can take on moisture and collapse into much more tightly packed "globules" (Mikhailov et al., 2006). These have greatly increased scattering and absorption cross-sections and greater forward scattering (Yin and Liu, 2010; Liu et al., 2012). Some recent discussions have focused on apparent discrepancy in absorption enhancement by the coating of BCFAs between measurement and models (Cappa et al., 2013). It has been noted that both the compactness and positioning of the BCFA within a coating medium have significant effects on mass absorbing cross-section (MAC) (Adachi et al., 2010; Scarnato et al., 2013)."

It would have been interesting a discussion of the authors numerical computations of absorptions properties of BC aggregates, which are not specifically addressed in the paper.

The numerical computations were carried out using MSTM with no bells

or whistles. This basically involved generating input files with the positions of each spherule in a BCFA defined, and passing this to MSTM along with refractive index and wavelength. To clarify this, the following sentence has been added after the first sentence in the methods section: "This required the input of individual spherule positions and radii within an aggregate, wavelength, and the refractive index."

3. I, personally, would find more "clear" having the equations that are currently in sec 3.3 and 3.4, instead presented in the method section, in this way there would be more space for discussion of results.

Initially these equations have been put in the Methods section, but we felt that the narrative of the paper was less clear in this form so changed to the current order. Discussion of results has been extended in response to several referee's comments, e.g. fitting of spheres in IR, additional comparisons with literature, conversion to MAC. These are highlighted elsewhere in this response.

4. In my opinion, generally, the results could be discussed more in the details and compared, where possible, with relevant literature. For example, results in fig, 2 and 3 could be compared with the work of Liu et al., 2008, Kahnert, 2010a,b; Kahnert and Devasthale, 2011; Wu et al., 2012, Scarnato et al, 2013.

Discussion has been increased. In particular, Figs. 2 & 3 and a new figure showing MAC at 550 nm are compared to several of the papers mentioned. e.g. "The mass absorption cross-section (MAC) is another common parameter used to describe black carbon aerosols. Values of MAC at $\lambda = 550\,\mathrm{nm}$ obtained by these calculations are shown in Fig. 4 and are consistent with similar calculations in the literature (Bond and Bergstrom, 2006; Kahnert, 2010a) which found calculated MAC values of around $6\,\mathrm{m^2/g}$. There is a discrepancy between this and measured values of MAC which are around $7.5\,\mathrm{m^2/g}$. Results also agree with the work of Scarnato et al. (2013) who found that 'lacy' aggregates had a higher MAC and lower SSA than more compact aggregates."

Discussion of other aspects of the results have been highlighted elsewhere in this response.

An increase in the font size in the plot would help in reading figures. Figures results are not discussed in detail in the text (for example Fig. 7).

Font sizes for Figures 2, 5, 6, and 7 have been increased. Discussion of the figures in the section "Finding appropriate spheres" has been greatly increased and is twice the length that it was previously. Explicit alterations are mentioned elsewhere in these responses, and we will also provide a copy of the altered manuscript showing all of our changes to the text highlighted.

Introduction section 1.2 page 3541: Line 3: Please, consider to rewrite the sentence Particles are defined by equation with Fractal aggregates can be described in terms of

Since the previous sentence refers to fractal aggregates, we have rewritten the sentence as: "They can be described in terms of the equation:"

Line 7: Please, consider to rewrite the sentence with the following: "The fractal dimension gives a measure of the compactness of the aggregate, a D_f value of 1 describe an open chain structure, while a D_f value of 3 describe a

compact aggregate"

Done. The sentence has been rewritten as: "The fractal dimension gives a measure of the compactness of an aggregate. A D_f value of 1 describes an open chain structure, whilst a D_f value of 3 describes a compact aggregate."

Line 22: instead of "correct" write "considered as reference values ". Remove quotations.

Done.

Method Please, explain the author choice to use different set of refractive indexes for different wavelengths ranges. Chang and Charalapopolous refractive index are provided, as well, in the 400 nm to 1um wavelength region.

While it is true that Chang and Charalapopolous' refractive index data extend down to 400 nm, the review paper by Bond and Bergstrom amalgamated these values along with many others into a best estimate of visible refractive index of BC lying along a "void fraction line" with their "best guess [being that] the high values [...] are the most promising." As such, we selected the B&B highest value of $1.95+0.79i$ and switched from C&C values to B&B values at the wavelength where this value intersected with the B&B value. This was between 1 and 2 μm. We acknowledge that this choice was a little ad hock but preferred it to a sudden discontinuity in RI that would have occurred if we had switched over at a different wavelength closer to the visible.

Results: The scattering cross section increase with increase of fractal dimension has also been found and discussed by Scarnato et al., (2013) and Liu et al. (2008), please add references.

A sentence discussing scattering cross-section in the first paragraph of the results section has been extended to read: "The scattering cross-section is more pronounced at higher D_f as the fractals become more densely packed and so a more coherent scattering entity as also reported by Liu et al. (2008); Scarnato et al. (2013)."

Response to the short comment by J. C. Corbin

1. A single value was used for the spherule radius a (25 nm). For atmospheric BCFAs, the value of a may vary considerably between different combustion sources. The current value of 25 nm would be representative of wood-combustion aerosol (Gwaze et al. 2006; Zelenay et al., 2011). Since diesel soot typically has smaller spherules about 7.520 nm in radius, with more-modern engines having smaller a (Burtscher, 2005) it would be interesting to see results or discussion on the impact of smaller a.

An interesting question. While we weren't able to run additional calculations in time for this response, previous studies by Kahnert (2010, AST) and Liu (2008, JQSRT) have found that in the visible, MAC is not affected by changes in spherule size $15 \leq a \leq 25$ nm while SSA decreases with smaller a. As a decreases, we would expect that the results would tend towards the Rayleigh limit at larger values of n_s and shorter λ, so it seems plausible to suggest that

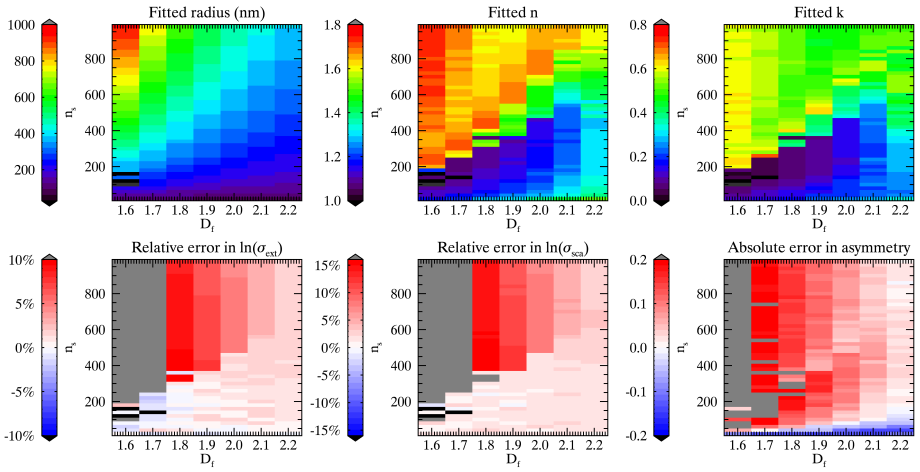

Figure R3: The optimum fitted sphere parameters (r, n, and k) and their resultant errors relative to the reference MSTM calculations in $\ln \sigma_{\text{ext}}$, $\ln \sigma_{\text{sca}}$ and g for BCFAs with $\lambda = 550\,\text{nm}$.

(ignoring changes in refractive index) optical properties will translate, to longer wavelengths and larger numbers of spherules for the same effect.

In the near future, we are intending to run calculations for the smaller values of a valid for diesel burning. For the purposes of this work, an additional comment has been added to the methods section, reading: "The burning of diesel fuels creates BCFAs with smaller spherules. More modern engines working in optimised combustion conditions can have spherules as small as $a = 6.5\,\text{nm}$, whilst emissions from black smoking diesel engines have sizes of $a = 17.5\,\text{nm}$ (Su, 2004). Future work will investigate the light scattering properties of these much smaller particles."

2. What was the motivation for choosing D_f as low as 1.6? Although this low value would reflect a DLCA-formed aggregate (Diffusion-Limited Cluster-Cluster Aggregation) of highly-polydisperse spherules (Eggersdorfer et al., 2012), to our knowledge natural soot aerosols have always been observed to consist of nearmonodisperse spherules so that $D_f = 1.8$ (Sorensen, 2011). This would be significant to Figs. 7 and 8, since the errors there are largest for the lowest D_f. The authors will probably agree that $D_f = 1.8$ is most relevant, as they have already focussed on this case in general.

We agree. It is very unlikely that BCFAs this open are seen often, although some BCFAs have been observed with D_f as low as 1.2 (Heinson, 2010). It was more an attempt to get a feel for how optical properties would change in an arbitrary fractal aggregate as it became more compact. The limits of error plots in Fig. 7 have been adjusted (see Fig. R3) so that the large errors from $D_f < 1.8$ are now beyond the scale of the colour bar. Even still, errors of > 10 % in both $\ln \sigma_{\text{ext}}$ and $\ln \sigma_{\text{sca}}$ are far too large to be acceptable. In order to keep $\ln \sigma$ errors below 5 % and g errors below 0.10, we would have to impose limits of $D_f \geq 1.8$ and $n_s < 100$.

3. As the authors have noted, the fractal dimension of soot particles may increase to 2.3 (Bambha et al., 2013) or higher (Zhang et al., 2008) following coating. The value of 2.3 is already outside the range of the D_f studied, presumably because the clustering algorithm does not represent subsequent restructuring. But since the coating-induced increase in D_f was prescribed during cluster formation and not afterwards, even the $D_f = 2.2$ aggregates may not have the same structure as restructured DLCA soot with $D_f = 2.2$. In particular, the anisotropy (Heinson et al. 2010; Eggersdorfer and Pratsinis, 2013) and fine structure (Mitchell et al., 2003) of restructured aggregates are not constrained by D_f alone. So the higher D_f values of restructured BCFAs may not be precisely captured by tuning the clustering algorithm to produce higher D_f values. This theoretical expectation is confirmed by a comparison of microscopy images (Bambha et al., 2013; Zhang et al., 2008) with the authors modelled BCFAs (shown in their Fig. 1). The modelled BCFAs appear to have a different, less-compact structure than the real restructured BCFAs. This would imply that the real restructured BCFAs may have smaller deviations from Mie theory than calculated in the manuscript. Would it be possible for the authors to somehow synthesize aggregates that are more spherical to provide an upper bound? We realize that this may be quite challenging without a quantitative restructuring model, but if the clustering algorithm is not representing the restructuring process, a manually-synthesized BCFA would not necessarily be less physical than the current high-D_f BCFAs.

It is definitely outside the scope of this work to attempt such restructuring or generating such a large number of particles manually, but we would be very interested in pursuing this avenue in future work. A short summary of the literature above has been added to the end of the section discussing fractal dimension (§1.2): It reads: "When aggregates collapse into more tightly packed, higher D_f clusters, they are restructured by the changes in humidity, and the coatings covering them. In these cases, the new shapes have formed in a fundamentally different manner from particles formed by the cluster-cluster algorithm used in this work (Thouy and Jullien, 1994) which gradually aggregates clusters to other clusters, never reordering previously added spherules within the aggregate. As such, the larger valued D_f aggregates should not be taken as realistic models for compact BCFAs after atmospheric processing. This can be seen in comparisons of real compact BCFAs (e.g. Mikhailov et al., 2006; Zhang et al., 2008; Bambha et al.,2013) with Fig. 1d generated by the cluster-cluster algorithm."

One final comment. Since the asymmetry parameter g was quite small for the smallest clusters (Fig. 5c, bottom row), perhaps it would be better in Fig. 7c to plot the absolute error in g instead of the relative error. The actual deviation here appears to be relatively small.

We agree, and this has been done.

We agree with Smith and Graingers conclusion that light-scattering by BCFAs cannot be accurately modelled as equivalent spheres in general, but we wonder whether this conclusion could be reversed under certain conditions: could the errors in an equivalent-sphere treatment in an atmospherically-relevant parameter space ($D_f > 1.8$ and $n_s < 500$) be small enough to be acceptable in at least some modelling applications?

As we mentioned above, in order to keep errors in $\ln \sigma$ below 5 % and errors in g below 0.10, we would have to impose limits of $D_f \geq 1.8$ and $n_s < 100$ which seems unacceptable for most modelling applications.

Response to the short comment by M. Kahnert

1. Comment on the results presented in Sect. 3.3: Similar work has been done and discussed in Kahnert, M.: Numerically exact computations of the optical properties of light absorbing carbon aggregates for wavelength of 200 nm - 12.2 um, Atmos. Chem. Phys. 10, 8319-8329, 2010. The fitting ansatz used there (Sect. 3.2) was slightly different from that proposed here and did not lend itself equally easily to analytically performing size integrations. In this regard the fitting approach proposed here by the authors is more useful. In the ACP paper by Kahnert the fitting approach was eventually dismissed and the computational results obtained for the black carbon aggregates were put into a look-up table and directly coupled to a chemical transport model and to a radiative transfer model. The rationale was that there really is no more need for parameterisations if one can perform aerosol optics calculations for all relevant sizes and wavelengths. That this is indeed possible has been demonstrated in that paper, and it has been confirmed by the work presented here by Smith and Grainger.

Agreed. In the methods section, we have added a passage commenting on the differences between our methods: "Similar work by (Kahnert (2010b) used fewer different sizes of BCFA, but attempted to find a "typical" geometry that was a good optical representation of BCFA at that size, by this method obtaining smoothly varying fields. In this study, only a single representation of each n_s and D_f particle was generated, and so one would expect occaisional outliers in the output optical properties. Since the aim of this work was to find a mapping of complex shapes to simple spherical equivalents it was thought that a parameterisation of the conversion would smooth out these issues."

In the results section, discussing the fitting, we have similiary compared our fitting strategies: "In the work of Kahnert (2010b), attempts to parameterise the optical properties σ_{abs} with a cubic polynomial in the radius of equal volume, r_v, were successful, but fits of σ_{sca}, $g \times \sigma_{\mathrm{sca}}$, and the backscatter cross-section were unsuccessful. Instead, fits to the logarithm of these quantities were obtained which made analytic integration over r_v to develop optical properties of size distibutions of BCFA unfeasible. As such, a look-up table of pre-computed BCFA optical properties was used instead. In this work, that problem is not encountered since we are dealing with parameters of the properties we desire to integrate directly."

2. Comment on comparison between modelling results and measurements: In the manuscript the authors mention that their modelled single-scattering albedo at visible wavelengths agrees well with observations as reviewed by Bond and Bergstrom (2006). However, Bond and Bergstrom also review measurements of the mass absorption cross section (MAC). The ACP paper by Kahnert (2010) cited above briefly mentions that existing computations for black carbon aggregates do not fully agree with available measurements. This problem is discussed in more detail by Kahnert M.: On the discrepancy between modeled and mea-

sured mass absorption cross sections of light absorbing carbon aerosols, Aerosol Sci. Technol. 44, 453-460, 2010. It would be interesting if the authors could convert their absorption cross section at 550 nm to MAC and compare to the measured values reviewed by Bond and Bergstrom, as well as to the computed values reported by Kahnert.

A very good idea. This has been done and a figure added to the paper showing MAC at 550 nm. We also include it here as Fig. R4. We find values of $5.8 < \mathrm{MAC} < 6.3$ for $\lambda = 550$ nm, $D_f = 1.8$ which is in agreement with your paper. Discussion of this has been added to the results section and reads: "The mass absorption cross-section (MAC) is another common parameter used to describe black carbon aerosols. Values of MAC at $\lambda = 550\,\mathrm{nm}$ obtained by these calculations are shown in Fig. 4 and are consistent with similar calculations in the literature (Bond and Bergstrom, 2006; Kahnert, 2010a) which found calculated MAC values of around $6\,\mathrm{m}^2/\mathrm{g}$. There is a discrepancy between this and measured values of MAC which are around $7.5\,\mathrm{m}^2/\mathrm{g}$. Results also agree with the work of Scarnato et al. (2013) who found that 'lacy' aggregates had a higher MAC and lower SSA than more compact aggregates."

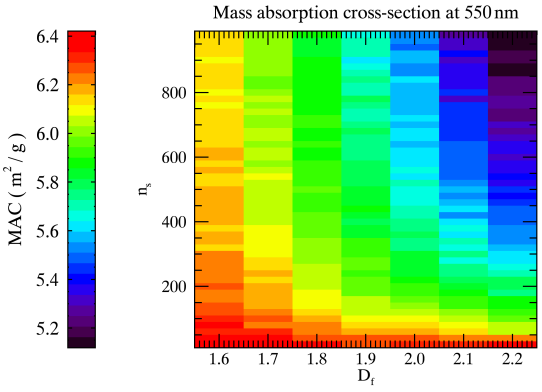

Figure R4: The mass absorption cross section at $\lambda = 550\,\mathrm{nm}$ for BCFAs. For these calculations, a density of $1.8\,\mathrm{g\,m^{-2}}$ was assumed. This figure has been added to the manuscript.

One more very minor thing: please correct the citation of Gustav Mies seminal paper: "Beiträgge" should be "Beiträge".

Done. Thank you for spotting this!

List of changes to the text

All changes are highlighted in the following copy of the manuscript.

P3540 L6: "fractal soot aerosol" → "**fractal BC aerosol**"

P3540 L10: "the soot emissions." → "**the BC emissions.**"

P3540 L16: "Although the soot spherules" → "**Although the BC spherules**"

P3540 L22: New paragraph after L22:

> "**Once the BCFAs become hydrophilic, they can take on moisture and collapse into much more tightly packed "globules" (Mikhailov et al., 2006). These have greatly increased scattering and absorption cross-sections and greater forward scattering (Yin and Liu, 2010; Liu et al., 2012). Some recent discussions have focused on apparent discrepancy in absorption enhancement by the coating of BCFAs between measurement and models (Cappa et al., 2012, 2013; Jacobson 2013). It has been noted that both the compactness and positioning of the BCFA within a coating medium have significant effects on mass absorbing cross-section (MAC) (Adachi et al., 2010; Scarnato et al., 2013).**"

P3541 L1: "Particles are defined by the equation" → "**They can be described in terms of the equation**"

P3541 L7—10: "The fractal dimension gives a measure of how "compact" an aggregate is, […] space between constituent parts)." → "**The fractal dimension gives a measure of the compactness of an aggregate. A Df value of 1 describes an open chain structure, whilst a Df value of 3 describes a compact aggregate.**"

P3541 L12 "such as soot" → "**such as BC**"

P3541 L22 " considered "correct". " → "**considered reference values.**"

P3541 L22: New paragraph after L22:

> "**An intermediate step between the rigour of MSTM and the simplicity of assuming spherical aerosols is Rayleigh-Debye-Gans theory (RDG) which assumes that the individual scattering spherules are small enough to be Rayleigh scatterers, and that these scatterers have a negligible multiple scattering interaction with each other. Further details can be found in the review paper by Sorensen (2001). However, as noted by Bond and Bergstrom (2006, §5.2 and references therein), several studies have shown an under-prediction of fractal aggregate absorption by RDG compared to rigorous light scattering calculations, particularly at longer wavelengths.**"

P3542 L3: Insert new sentence at the full stop: **"This required the input of individual spherule positions and radii within an aggregate, wavelength, and the refractive index.**"

P3542 L6: Insert new sentences at the full stop, and the new paragraph at the end:

> "**The spherule radius of 25 nm is representative of wood combustion aerosol (Gwaze et al., 2006) and has been noted to give the best agreement in single scatter albedo between measurements and calculations (Kahnert, 2010a). The burning of diesel fuels creates BCFAs with smaller spherules. More modern engines working in optimised combustion conditions can have spherules as small as a = 6.5nm, whilst emissions from black smoking diesel engines have sizes of a = 17.5nm (Su et al., 2004). Future work will investigate the light scattering properties of these much smaller particles. [NEW PARAGRAPH]**"

P3542 L11: Insert new sentences at the full stop:

"**Similar work by Kahnert (2012b) used fewer different sizes of BCFA, but attempted to find a "typical" geometry that was a good optical representation of BCFA at that size, by this method obtaining smoothly varying fields. In this study, only a single representation of each ns and Df particle was generated, and so one would expect occasional outliers in the output optical properties. Since the aim of this work was to find a mapping of complex shapes to simple spherical equivalents it was thought that a parameterisation of the conversion would smooth out these issues.**"

P3542 L15: Added new reference: "(e.g. Stier et al., 2007)" → "**(e.g. Stier et al., 2007; Kahnert, 2012b)**"

P3542 L19: New paragraph added at the end of the sentence:

"**When aggregates collapse into more tightly packed, higher Df clusters, they are restructured by the changes in humidity, and the coatings covering them. In these cases, the new shapes have formed in a fundamentally different manner from particles formed by the cluster-cluster algorithm used in this work (Thouy and Jullien, 1994) which gradually aggregates clusters to other clusters, never reordering previously added spherules within the aggregate. As such, the larger valued Df aggregates should not be taken as realistic models for compact BCFAs after atmospheric processing. This can be seen in comparisons of real compact BCFAs (e.g. Mikhailov et al., 2006; Zhang et al., 2008; Bambha et al., 2013) with Fig. 1d generated by the cluster-cluster algorithm.**"

P3543 L2: Added to end of sentence: "...scattering entity." → "...**scattering entity as also reported by Liu et al. (2008); Scarnato et al. (2013).**"

P3543 L7: Added new sentences after the full stop:

"**The mass absorption cross-section (MAC) is another common parameter used to describe black carbon aerosols. Values of MAC at λ = 550nm obtained by these calculations are shown in Fig. 4 and are consistent with similar calculations in the literature (Bond and Bergstrom, 2006; Kahnert, 2010a) which found calculated MAC values of around $6m^2$=g. There is a discrepancy between this and measured values of MAC which are around $7.5m^2$=g. Results also agree with the work of Scarnato et al. (2013) who found that "lacy" aggregates had a higher MAC and lower SSA than more compact aggregates.**"

P3544 L5—6: Remove new paragraph. Change subsequent start of sentence: "Relative errors..." → "**We see relative errors**..."

P3544 L8: Added new sentence after the full stop:

"**Additionally, sudden discontinuities in the fitted refractive index show that a regime change based on particle size would be required.**"

P3544 L9: New paragraph inserted after second sentence:

"**One might expect that at longer wavelengths as the scattering BCFAs approached the Rayleigh limit, the ability to fit spheres would improve. However, the asymmetry parameter at these wavelengths is non-negligible for the less compact and larger BCFAs (unlike Rayleigh scatterers) as can be seen in Figures 6 and 7. This means that it is not possible to find spheres that can match $\ln\sigma_{ext}$ and $\ln\sigma_{sca}$, whilst also having a large enough g. As such, a trade off between large errors in either the cross-sections, or asymmetry must be made. The fit with large errors in g is shown in Fig. 9.**"

P3544 L12: New sentence added at the end of the paragraph:

"**Earlier work by Li et al. (2010) had found that it was not possible to represent the phase**

function for a reasonable size distribution of BCFAs with a similar distribution of spheres at wavelengths of λ = 0.628 and 1.1 μm, so even had a good fit of σ_{ext}, σ_{sca}, and g been found, it is unlikely that the full phase function resulting would have been appropriate."

P3545 L8: New paragraph added:

"**In the work of Kahnert (2012b), attempts to parameterise the optical properties σ_{abs} with a cubic polynomial in the radius of equal volume, rv, were successful, but fits of σ_{sca}, g x σ_{sca}, and the backscatter cross-section were unsuccessful. Instead, fits to the logarithm of these quantities were obtained which made analytic integration over r_v to develop optical properties of size distributions of BCFA infeasible. As such, a look-up table of pre-computed BCFA optical properties was used instead. In this work, that problem is not encountered since we are dealing with parameters of the properties we desire to integrate directly.**"

P3548 L6: New sentence added after full stop: "**Other approximations such as RDG can improve greatly the representation of BCFA optical properties but generally do not provide sufficient absorption.**"

P3548 L9: New sentence added after full stop: **"Uncertainties in the size distribution, shape, and composition of these particles should not be forgotten and will certainly cause differences at least as large as the simplification of optical properties to spheres or RDG.**"

P3551 L22: "Beiträgge" → "**Beiträge**"

P3553 Caption: Additional sentence added at the end of the caption: "**While the values of coefficient 1 (the linear term) in the fits of SSA and g are negligible at 550 nm, they increase at longer wavelengths while the values of coefficient 2 (the logarithmic term) decrease.**"

P3554 Caption: "N=300" → "n_s=300" to match notation in main text.

P3560 Caption: Changed to

"**The optimum fitted sphere parameters (r, n, and k) and their resultant errors relative to the reference MSTM calculations in $\ln\sigma_{ext}$, $\ln\sigma_{sca}$ and absolute errors in g for BCFAs with λ = 550nm. The colour scale has been adjusted so that the very large errors caused by unphysically small BCFA Df are clipped.**"

P3562 Caption: Following sentences added to the end of the caption:

"**The MSTM calculations (Data) are blue, the fitted data for the same radii (Fit) are orange, and the missing area covered by the fit, but not the MSTM calculations (Missing) are red. Numbers in these colours give the area under the respective curves. Δ gives the difference in areas between Data and Fit. The missing fraction is the fractional volume of Fit, not covered by Data.**"

Changes to figures

- Figure 2 has been updated (size of font, position of colour bar).
- A new figure has been added as Figure 3 showing MAC at 550 nm.
- Figure 4 is now Figure 5.
- Figure 5 has been updated (size of font, position of colour bar) and is now Figure 6.
- Figure 6 has been updated (size of sont, position of colour bar) and is now Figure 7.
- Figure 7 has been updated (size of font, position of colour bar, range of colour bars, absolute

error in g instead of relative error in g) and is now Figure 8.

- A new figure has been added as Figure 9, replicating results of Figure 8, at 12um.
- Figure 8 is now Figure 10.
- Figure 9 is now Figure 11.

Added references

Adachi, K., Chung, S. H., and Buseck, P. R.: Shapes of soot aerosol particles and implications for their effects on climate, J. Geophys. Res., 115, D15206, doi:10.1029/2009JD012868, 2010.

Bambha, R. P., Dansson, M. A., Schrader, P. E., and Michelsen, H. A.: Effects of volatile coatings on the laser-induced incandescence of soot, Appl. Phys. B, 112, 343–358, doi:10.1007/s00340-013-5463-9, 2013.

Cappa, C. D., Onasch, T. B., Massoli, P., Worsnop, D. R., Bates, T. S., Cross, E. S., Davidovits, P., Hakala, J., Hayden, K. L., Jobson, B. T., Kolesar, K. R., Lack, D. A., Lerner, B. M., Li, S.-M., Mellon, D., Nuaaman, I., Olfert, J. S., Pet¨aj¨a, T., Quinn, P. K., Song, C., Subramanian, R., Williams, E. J., and Zaveri, R. A.: Radiative Absorption Enhancements Due to the Mixing State of Atmospheric Black Carbon, Science, 337, 1078-1081, doi:10.1126/science.1223447, 2012.

Cappa, C. D., Onasch, T. B., Massoli, P., Worsnop, D. R., Bates, T. S., Cross, E. S., Davidovits, P., Hakala, J., Hayden, K. L., Jobson, B. T., Kolesar, K. R., Lack, D. A., Lerner, B. M., Li, S.-M., Mellon, D., Nuaaman, I., Olfert, J. S., Pet¨aj¨a, T., Quinn, P. K., Song, C., Subramanian, R., Williams, E. J., and Zaveri, R. A.: Response to Comment on "Radiative Absorption Enhancements Due to the Mixing State of Atmospheric Black Carbon", Science, 339, 393, doi:10.1126/science.1230260, 2013.

Gwaze, P., Schmid, O., Annegarn, H. J., Andreae, M. O., Huth, J. and Helas, G.: Comparison of three methods of fractal analysis applied to soot aggregates from wood combustion, J. Aerosol Sci., 37, 820–838, doi:10.1016/j.jaerosci.2005.06.007, 2006.

Jacobson, M. Z.: Comment on "Radiative Absorption Enhancements Due to the Mixing State of Atmospheric Black Carbon", Science, 339, 393, doi:10.1126/science.1229920, 2013.

Kahnert, M.: On the Discrepancy between Modeled and Measured Mass Absorption Cross Sections of Light Absorbing Carbon Aerosols, Aerosol Sci. Tech., 44, 453–460, doi:10.1080/02786821003733834, 2010a.

Kahnert, M.: Numerically exact computation of the optical properties of light absorbing carbon aggregates for wavelength of 200nm–12.2 μm. Atmos. Chem. Phys., 10, 8319-–8329, 44, 453–460, doi:10.5194/acp-10-8319-2010, 2010b.

Liu, L., Mishchenko, M. I., and Arnott, W. P.: A study of radiative properties of fractal soot aggregates using the superposition T-matrix method, J. Quant. Spectrosc. Ra., 109, 2656–2663, doi:10.1016/j.jqsrt.2008.05.001, 2008.

Liu, C., Panetta, R. L., and Yang, P.: The Influence ofWater Coating on the Optical Scattering Properties of Fractal Soot Aggregates, Aerosol Sci. Tech., 46, 31–43, doi:10.1080/02786826.2011.605401, 2012.

Mikhailov, E. F., Vlasenko, S. S., Podgorny, I. A., Ramanathan, V., and Corrigan, C. E.: Optical properties of soot–water drop agglomerates: An experimental study, J. Geophys. Res., 111, D07209, doi:10.1029/2005JD006389, 2006.

Scarnato, B. V., Vahidinia, S., Richard, D. T., and Kirchstetter, T. W.: Effects of internal mixing and aggregate morphology on optical properties of black carbon using a discrete dipole approximation model, Atmos. Chem. Phys., 13, 5089, doi:10.5194/acp-13-5089-2013, 2013.

Su, D. S., M¨uller, J.-O., Jentoft, R. E., Rothe, D., Jacob, E. and Schl¨ogl, R.: Fullerene-like soot from EuroIV diesel engine: consequences for catalytic automotive pollution control, Top. Catal., 30–31, 241–245, doi:10.1023/B:TOCA.0000029756.50941.02, 2004.

Yin, J. Y. and Liu, L. H.: Influence of complex component and particle polydispersity on radiative properties of soot aggregate in atmosphere, J. Quant. Spectrosc. Ra., 111, 2115–2126, doi:10.1016/j.jqsrt.2010.05.016, 2010.

Manuscript prepared for Atmos. Chem. Phys. Discuss.
with version 4.1 of the LaTeX class copernicus_discussions.cls.
Date: 2 June 2014

Simplifying the calculation of light scattering properties for black carbon fractal aggregates

A. J. A. Smith and R. G. Grainger

Atmospheric, Oceanic and Planetary Physics, Clarendon Laboratory, Oxford, OX1 3PU, UK

Correspondence to: A. J. A. Smith (smith@atm.ox.ac.uk)

Abstract

Black carbon fractal aggregates have complicated shapes that make the calculation of their optical properties particularly computationally expensive. Here, a method is presented to estimate fractal aggregate light scattering properties by optimising simplified models to full light scattering calculations. It is found that there are no possible spherical models (at any size or refractive index) that well represent the light scattering in the visible, or near-thermal infrared. As such, parameterisations of the light scattering as a function of the number of aggregate particles is presented as the most pragmatic choice for modelling distributions of black carbon when the large computational overheads of rigorous scattering calculations cannot be justified. This parameterisation can be analytically integrated to provide light scattering properties for log-normal distributions of black carbon fractal aggregates and return extinction cross-sections with 0.1 % accuracy for typical black carbon size distributions. Scattering cross-sections and the asymmetry parameter can be obtained to within 3 %.

1 Introduction

Particulate products of incomplete combustion, such as black carbon (BC), have been the subject of recent intense discussion (e.g. Jacobson, 2002, 2003; Bond, 2007; Bond et al., 2013). Emissions rates are high (Bond et al., 2004), and have tripled in the last 140 yr (Ito and Penner, 2005) although specific regions have not followed this trend. The developed world has reduced emissions while Asian countries have come to dominate carbon aerosol emission (Streets et al., 2003). Since BC has a high imaginary part of refractive index, it is one of the few aerosols that has a positive direct effect on radiative forcing (Jacobson, 2001; Bond, 2007; Bahadur et al., 2011).

Studies have shown that when BC is deposited on snow, the lowering of surface albedo leads to faster run-off and to an additional warming effect (e.g. Flanner et al., 2009; Doherty et al., 2010), although other absorbing aerosols also play a role (Bond et al., 2013). Aside from the positive radiative forcing due to BC, there are considerable negative health effects from fine

particulate matter (Dockery et al., 1993; Jansen et al., 2005), and in urban environments, issues of poor visibility (Larson et al., 1989).

Black carbon fractal aggregates (BCFA) are clusters of BC spherules forming aerosols with a non-spherical shape. Accurate quantification of their optical properties is important both for their measurement, and for predicting their radiative effect. Current estimates of the climate forcing caused by BC emissions are positive with a typical value of $1.1\,\mathrm{W\,m^{-2}}$ (Bond et al., 2013).

The object of this work is to see whether there are spheres (of some radius, r and complex refractive index, m) whose optical properties are close enough to a BCFA's light scattering properties (as calculated using T-Matrix code) to acceptably represent these particles. If some mapping of r and m to properties of the BCFA can be found, there may be additional physical insight into the fractal light scattering, additional to the advantage of a much simpler scattering calculation.

After a brief description of black carbon, we show that this is not possible within the bounds of reasonably sized spheres with a wide range of refractive indices and go on to present a parameterisation of BCFA light scattering properties.

1.1 A physical description of aerosol formation and ageing

Formation of sub-micron aggregate aerosols from burning is a rapid process involving several stages, some of which are irreversible. Initially, due to very high temperatures, some of the burning fuel vapourises (if it is not already gaseous). If the fuel is something such as coal, the main products could be inorganics and elemental carbon formed from the vapouried coal ash (Helble et al., 1988; Turns, 2000). In the case of biomass, this could be organics such as benzene and poly-aromatic hydrocarbons (PAH) (Reid et al., 2005).

Further away from the hottest part of the flame, nucleation of these molecules leads to the formation of very small particles with diameters of 1–2 nm (Calcote, 1981). These quickly grow by coagulation and surface condensation to sizes of 10–30 nm. Coagulation is encouraged initially due to a high proportion of hydrocarbon radicals which falls off as the particles age (Homann, 1967; Calcote, 1981). High resolution TEM images of individual carbonaceous spherules shows

them to be haphazardly ordered micro-structures of graphene-like layers (Buseck et al., 1987; Pósfai et al., 1999; Li et al., 2003) with a very narrow range of diameters for a specific flame (Homann, 1967).

After the initial nucleation and coagulation, primary particles can aggregate leading to the fractal BC aerosol often seen (e.g. Helble et al., 1988; Sorensen, 2001; Li et al., 2003; Zhang et al., 2008). As the particles pass through the edge of the flame, some will be oxidised, although not completely (Turns, 2000). Those that make it through the flame without burning are the BC emissions. Flames that burn more intensely have poorer transport of oxygen into the area where the particles are being created, and as a result will emit more particulate matter (Reid et al., 2005).

The aggregates created during burning last a very short amount of time, of the order of hours (Martins et al., 1998b), before being irreversibly deformed as the chain-like structures fold up into more spherical clusters (Martins et al., 1998a; Abel et al., 2003). Although the BC spherules are hydrophobic, their irregular shapes provide active sites where water can be deposited (Zhang et al., 2008). This change is thought to be due to atmospheric processing of the particles by nucleating water, and the coating of the carbon by nucleating additional products of the burning, e.g. sulphate and OC. This also means that the BC cores become coated in shells of other material which are generally hydrophilic (Popovicheva et al., 2008). This coating enhances the light absorption of the BC core (Fuller et al., 1999; Jacobson, 2001; Bond et al., 2006).

Once the BCFAs become hydrophilic, they can take on moisture and collapse into much more tightly packed "globules" (Mikhailov et al., 2006). These have greatly increased scattering and absorption cross-sections and greater forward scattering (Yin and Liu, 2010; Liu et al., 2012). Some recent discussions have focused on apparent discrepancy in absorption enhancement by the coating of BCFAs between measurement and models (Cappa et al., 2012, 2013; Jacobson, 2013). It has been noted that both the compactness and positioning of the BCFA within a coating medium have significant effects on mass absorbing cross-section (MAC) (Adachi et al., 2010; Scarnato et al., 2013).

1.2 Fractal dimension

Fractal aggregate particles are to some extent scale invariant, although do not have the true scale invariance of a mathematical fractal, which would have infinite extent. They can be described in terms of the equation

$$n_{\mathrm{s}} = k_{\mathrm{f}} \left(\frac{R_{\mathrm{g}}}{a} \right)^{D_{\mathrm{f}}}, \tag{1}$$

where n_{s} is the number of spherules in the aggregate, a is the radius of an individual spherule in the fractal, D_{f} is the fractal dimension, k_{f} is the fractal prefactor, and R_{g} is the radius of gyration which gives the root-mean-square distance of spherules from the cluster's centre of mass (Sorensen, 2001).

The fractal dimension gives a measure of the compactness of an aggregate. A D_{f} value of 1 describes an open chain structure, whilst a D_{f} value of 3 describes a compact aggregate. This dependence of shape on D_{f} is shown in Fig. 1.

For particles formed by diffusion limited cluster aggregation (such as BC from flames), fractal dimensions of $D_{\mathrm{f}} \simeq 1.75 \rightarrow 1.8$ are expected (Sorensen, 2001).

1.3 Light scattering methods

The scattering of light by a spherical particle can be solved analytically using Mie's solution to Maxwell's equations (Mie, 1908; Bohren and Huffman, 1983). Additionally, the derivatives of all light scattering properties are also analytic (Grainger et al., 2004).

The scattering of light by fractal clusters can be calculated using the Multiple Spheres T-Matrix Fortran-90 code (MSTM) (Mackowski, 2012) which is based on theory found in Mackowski and Mishchenko (1996). This method combines the spherical wave expansions for each spherule (at that spherules origin) in the aggregate, and orientationally averages. For this work, the results from this method are considered reference values.

An intermediate step between the rigour of MSTM and the simplicity of assuming spherical aerosols is Rayleigh-Debye-Gans theory (RDG) which assumes that the indi-

vidual scattering spherules are small enough to be Rayleigh scatterers, and that these scatterers have a negligible multiple scattering interaction with each other. Further details can be found in the review paper by Sorensen (2001). However, as noted by Bond and Bergstrom (2006, §5.2 and references therein), several studies have shown an underprediction of fractal aggregate absorption by RDG compared to rigorous light scattering calculations, particularly at longer wavelengths.

2 Method

Light scattering properties of BCFAs were calculated over a range of wavelengths, λ, from 400 nm to 15 µm using the MSTM code. This required the input of individual spherule positions and radii within an aggregate, wavelength, and the refractive index. The fractal aggregates were generated using a cluster–cluster algorithm (Thouy and Jullien, 1994) with a spherule radius of 25 nm and fixed fractal prefactor of $k_{\mathrm{f}} = 1.18$ which is very close to value used by Liu and Mishchenko (2005); Zhao and Ma (2009); Li et al. (2010). The spherule radius of 25 nm is representative of wood combustion aerosol (Gwaze et al., 2006) and has been noted to give the best agreement in single scatter albedo between measurements and calculations (Kahnert, 2010a). The burning of diesel fuels creates BCFAs with smaller spherules. More modern engines working in optimised combustion conditions can have spherules as small as $a = 6.5$ nm, whilst emissions from black smoking diesel engines have sizes of $a = 17.5$ nm (Su et al., 2004). Future work will investigate the light scattering properties of these much smaller particles.

For $400\,\mathrm{nm} \leq \lambda \leq 1\,\mu\mathrm{m}$, a step size of $\Delta\lambda = 150$ nm and a fixed refractive index of $m_{\mathrm{BC}} = 1.95 + 0.79i$ was selected, following Bond and Bergstrom (2006). Above this, the step size was widened to $\Delta\lambda = 1$ µm and a parameterised refractive index fit by Chang and Charalampopoulos (1990) was used. To alter the shape and size, the number of spherules was varied in steps of 20 with $20 \leq n_{\mathrm{s}} \leq 980$ and fractal dimension in steps of 0.1 with $1.6 \leq D_{\mathrm{f}} \leq 2.2$. Similar work by Kahnert (2012b) used fewer different sizes of BCFA, but attempted to find a "typical" geometry that was a good optical representation of BCFA at that size, by this method obtaining smoothly varying fields. In this study, only a single representation of each n_s and D_f particle

was generated, and so one would expect occasional outliers in the output optical properties. Since the aim of this work was to find a mapping of complex shapes to simple spherical equivalents it was thought that a parameterisation of the conversion would smooth out these issues. The calculated optical properties were the extinction and scattering cross-sections, σ_{ext}, σ_{sca}, and the asymmetry parameter g which gives a measure of the angular distribution of scattered light (Bohren and Huffman, 1983) and is used in several global circulation models to represent aerosol optical properties (e.g. Stier et al., 2007; Kahnert, 2012b).

Next, best fits of spherical radius and complex refractive index ($m = n + ik$) of spheres were fitted to the individual BCFAs. Optimal estimation (Rodgers, 2000) and least-squares fitting were tried. The differential optical properties required for the inversion, e.g. $\frac{\partial \sigma_{\text{ext}}}{\partial r}$, $\frac{\partial g}{\partial n}$, were obtained using IDL code described in Grainger et al. (2004).

When aggregates collapse into more tightly packed, higher D_f clusters, they are restructured by the changes in humidity, and the coatings covering them. In these cases, the new shapes have formed in a fundamentally different manner from particles formed by the cluster-cluster algorithm used in this work (Thouy and Jullien, 1994) which gradually aggregates clusters to other clusters, never reordering previously added spherules within the aggregate. As such, the larger valued D_f aggregates should not be taken as realistic models for compact BCFAs after atmospheric processing. This can be seen in comparisons of real compact BCFAs (e.g. Mikhailov et al., 2006; Zhang et al., 2008; Bambha et al., 2013) with Fig. 1d generated by the cluster-cluster algorithm.

3 Results

3.1 Optical properties of black carbon fractal aggregates

Figure 2 shows the extinction and scattering cross-sections, and asymmetry parameter for BCFAs as a function of D_{f} and n_{s} in the visible. Although not clear from the figure (due to the logarithmic scale), the extinction cross-section is broadly a function of the particle volume suggesting that using the Rayleigh limit might be appropriate. The scattering cross-section is more

pronounced at higher D_f as the fractals become more densely packed and so a more coherent scattering entity as also reported by Liu et al. (2008); Scarnato et al. (2013). Similarly, g shows a greated amount of the light being scattered forwards as the fractals become both more densely packed, and larger.

Figure 3 shows the single scatter albedo (SSA $= \sigma_{sca}/\sigma_{ext}$) which agrees well with the literature review by Bond and Bergstrom (2006), who noted that when measured, the SSA of BCFAs are "surprisingly consistent" with a value of 0.2–0.3. The mass absorption cross-section (MAC) is another common parameter used to describe black carbon aerosols. Values of MAC at $\lambda = 550\,\mathrm{nm}$ obtained by these calculations are shown in Fig. 4 and are consistent with similar calculations in the literature (Bond and Bergstrom, 2006; Kahnert, 2010a) which found calculated MAC values of around $6\,\mathrm{m^2/g}$. There is a discrepancy between this and measured values of MAC which are around $7.5\,\mathrm{m^2/g}$. Results also agree with the work of Scarnato et al. (2013) who found that "lacy" aggregates had a higher MAC and lower SSA than more compact aggregates.

Since fractal aggregates are by nature randomly assembled, these are not the only possible representations of the light scattering properties that a BCFA with these properties could have. However, as shown in Fig. 5, relative difference from the mean values of the three parameters are small, with variance in the total extincion generally less than 1 % away from the mean, and less than 5 % away for σ_{sca} and g at $\lambda = 550\,\mathrm{nm}$.

At $\lambda = 12\,\mu\mathrm{m}$, one might expect things to be more straightforward. The size parameter of the largest BCFAs studied are $x_V = 0.1$ and $x_G = 0.6$ (by equivalent volume and radius of gyration respectively) which would place the vast majority of studied equivalent spherical particles in the Rayleigh limit. In that case it would be expected that $g \simeq 0$ and that there would be little dependency of the cross-sections with shape. Figure 6 shows BCFA light scattering at $12\,\mu\mathrm{m}$, where the refractive index is $m_{BC} = 2.93 + 2.16i$. For particles with large D_f values, the asymmetry is close to zero, but this is not the case for larger particles with smaller fractal dimensions.

The calculations over the entire wavelength range are shown in Fig. 7 at a fixed fractal dimension of $D_f = 1.8$. Extinction cross-sections decrease with decreasing size parameter (either

because of increasing wavelength or decreasing numbers of spherules in the aggregate). Single scatter albedo and asymmetry also decrease with decreasing size parameter and increasing k.

3.2 Finding appropriate spheres

For all of the BCFAs, it was attempted to find matching optical properties using spheres with $50 < r < 1500\,\mathrm{nm}$, $1 < n < 4$, and $0 < k < 4$. Attempting to fit closest values of $\ln\sigma_{\mathrm{ext}}$, $\ln\sigma_{\mathrm{sca}}$, and g using optimal estimation (Rodgers, 2000) is shown in Fig. 8 for $\lambda = 550\,\mathrm{nm}$. We see relative errors of $> 15\,\%$ for extinction, $> 20\,\%$ for scattering, and $> 40\,\%$ for asymmetry at this wavelength which are unacceptable, and do not improve with increased wavelength. Additionally, sudden discontinuities in the fitted refractive index show that a regime change based on particle size would be required. Similar attempts fitting the single scatter albedo instead of $\ln\sigma_{\mathrm{sca}}$, and σ instead of $\ln\sigma$ values also were not successful. Least-square fits were also unsuccessful.

One might expect that at longer wavelengths as the scattering BCFAs approached the Rayleigh limit, the ability to fit spheres would improve. However, the asymmetry parameter at these wavelengths is non-negligible for the less compact and larger BCFAs (unlike Rayleigh scatterers) as can be seen in Figures 6 and 7. This means that it is not possible to find spheres that can match $\ln\sigma_{\mathrm{ext}}$ and $\ln\sigma_{\mathrm{sca}}$, whilst also having a large enough g. As such, a trade off between large errors in either the cross-sections, or asymmetry must be made. The fit with large errors in g is shown in Fig. 9.

As such, it is suggested that within the range $0.4 \leq \lambda \leq 15\,\mu\mathrm{m}$, there are no suitable sizes or refractive indices of spheres appropriate for the optical modelling of black carbon aggregates. Earlier work by Li et al. (2010) had found that it was not possible to represent the phase function for a reasonable size distribution of BCFAs with a similar distribution of spheres at wavelengths of $\lambda = 0.628$ and $1.1\,\mu\mathrm{m}$, so even had a good fit of σ_{ext}, σ_{sca}, and g been found, it is unlikely that the full phase function resulting would have been appropriate.

3.3 Parameterising fractal aggregate optical properties

Since the extinction cross-section scales with volume which is proportional to n_s, a polynomial in n_s was chosen and order 3 was found to adequately capture the full range of λ, D_f and n_s used here.

$$\sigma_\mathrm{ext} = \sum_{m=0}^{3} k_m \, n_\mathrm{s}^m. \tag{2}$$

The scattering cross-section is not so simple to parameterise, and so the SSA is fitted instead and multiplied by σ_ext to obtain σ_sca. The SSA and g are both well captured by a logarithmic n_s and a linear offset. This was due to the tendency of these optical properties to initially increase with n_s before levelling off at large n_s:

$$\mathrm{SSA} = w_0 + w_1 \, n_\mathrm{s} + w_2 \ln n_\mathrm{s}, \tag{3}$$

$$g = G_0 + G_1 \, n_\mathrm{s} + G_2 \ln n_\mathrm{s}. \tag{4}$$

Table 1 shows the fit coefficients at $550\,\mathrm{nm}$ and $D_\mathrm{f} = 1.8$. The root-mean-square (RMS) errors in σ_ext, SSA, and g compared to the calculated values are also given. Including the smallest particles is roughly responsible for a doubling in the error of the fits, as can be shown by not including the two smallest particle sizes in the calculation. This is because the limit $\lim_{n_\mathrm{s}\to 0}(\sigma_\mathrm{ext}) = 0$ and $\lim_{n_\mathrm{s}\to 0}(g) = 0$ leading to large inflation in the relative differences between points. Over the entire range of λ and D_f, errors in the visible are below 3 % as shown in Fig. 10. In the range $2 \leq \lambda \leq 9\,\mu\mathrm{m}$, RMS errors in SSA and g can be as large as 10 %. Errors in extinction are $< 10\,\%$ in all cases.

In the work of Kahnert (2012b), attempts to parameterise the optical properties σ_abs with a cubic polynomial in the radius of equal volume, r_v, were successful, but fits of σ_sca, $g \times \sigma_\mathrm{sca}$, and the backscatter cross-section were unsuccessful. Instead, fits to the logarithm of these quantities were obtained which made analytic integration over r_v to develop optical properties of size distributions of BCFA infeasible. As such, a look-up table of pre-computed BCFA optical properties was used instead. In this work, that problem is not encountered since we are dealing with parameters of the properties we desire to integrate directly.

3.4 Parameterising light scattering for a lognormal distribution of particles

From these fitted optical schemes, the optical properties of lognormal distributions of these particles can be obtained trivially. For the extinction, we first relate n_s to a size distribution by volume-equivalent radius, r, saying

$$r = a\sqrt[3]{n_\mathrm{s}}, \tag{5}$$

and inserting into a lognormal distribution defined as:

$$n(r) = \frac{N}{\sigma r\sqrt{2\pi}} \exp\left[-\frac{1}{2}\left(\frac{\ln r - \ln r_0}{\sigma}\right)^2\right], \tag{6}$$

where N is the total number of particles in the distribution, σ is the standard deviation of $\ln r$, and r_0 is the geometric mean of r. The extinction coefficient at some point along the path of a light beam, z, is defined as

$$\beta_\mathrm{ext}(z) = \int_0^\infty \sigma_\mathrm{ext}(r)\, n(r,z)\, \mathrm{d}r. \tag{7}$$

Following from Eq. (2), σ_ext can separated into four terms in powers of r^3:

$$\sigma_\mathrm{ext} = \sum_{i=0}^{3} k_m \left(\frac{r}{a}\right)^{3m}. \tag{8}$$

Finally, noting that

$$\frac{1}{\sigma\sqrt{2\pi}} \int_0^\infty r^{m-1} \exp\left[-\frac{1}{2}\left(\frac{\ln\frac{r}{r_0}}{\sigma}\right)^2\right] \mathrm{d}r = r_0^m e^{\frac{m^2\sigma^2}{2}}, \tag{9}$$

an expression for β_{ext} is given by

$$\beta_{\text{ext}} = N \sum_{m=0}^{3} k_m \left(\frac{r_0}{a}\right)^{3m} e^{\frac{(3m\sigma)^2}{2}}. \tag{10}$$

Scattering is obtained from the extinction and single scatter albedo as:

$$\begin{aligned}\beta_{\text{sca}}(z) &= \int_0^\infty \sigma_{\text{sca}}(r)\, n(r,z)\, \mathrm{d}r = \int_0^\infty \sigma_{\text{ext}}(r)\, \text{SSA}(r)\, n(r,z)\, \mathrm{d}r, \\ &= \int_0^\infty \sum_{m=0}^{3} k_m \left(\frac{r}{a}\right)^{3m} \left[w_0 + w_1 \left(\frac{r}{a}\right)^3 + w_2 \ln\left(\frac{r}{a}\right)^3\right] n(r,z)\mathrm{d}r. \end{aligned} \tag{11}$$

Using

$$\frac{1}{\sigma\sqrt{2\pi}} \int_0^\infty r^{m-1} \ln r \exp\left[-\frac{1}{2}\left(\frac{\ln\frac{r}{r_0}}{\sigma}\right)^2\right] \mathrm{d}r = r_0^m e^{\frac{m^2\sigma^2}{2}} \left(\ln r_0 + m\sigma^2\right), \tag{12}$$

this can be reduced to

$$\begin{aligned}\beta_{\text{sca}} &= N\beta_{\text{ext}} \left(w_0 - 3w_2 \ln a\right) \\ &\quad + N \sum_{m=0}^{3} k_m \left(\frac{r_0}{a}\right)^{3m} e^{\frac{(3m\sigma)^2}{2}} \times \left[w_1 \left(\frac{r_0}{a}\right)^3 e^{\frac{9\sigma^2(2m+1)}{2}} + 3w_2 \left(\ln r_0 + 3m\sigma\right)\right]. \end{aligned} \tag{13}$$

Similar integration can be used to find the averaged asymmetry parameter for the size distribution, $< g >$, using:

$$< g >= \frac{\int_0^\infty \sigma_{\text{sca}}(r)\, g(r)\, n(r,z)\, \mathrm{d}r}{\beta_{\text{sca}}}, \tag{14}$$

by noting that:

$$\frac{1}{\sigma\sqrt{2\pi}}\int_0^\infty r^{m-1}\ln^2 r\exp\left[-\frac{1}{2}\left(\frac{\ln\frac{r}{r_0}}{\sigma}\right)^2\right]\mathrm{d}r = r_0^m e^{\frac{m^2\sigma^2}{2}}\left[(\ln r_0 + m\sigma^2)^2+\sigma^2\right]. \quad (15)$$

Using a reasonable atmospheric BC size distribution ($r_0 = 120\,\mathrm{nm}$; $\sigma = \ln 1.32$), differences between the extinction calculated by summing the various individual fractal calculations, and the parameterisation were investigated. The method used is shown for the example of $\lambda = 2\,\mu\mathrm{m}$ and $D_\mathrm{f} = 1.8$ in Fig. 11. The parameterisation is an integral over the whole of particle radius space, whereas the calculations of fractal optical properties were truncated at $n_\mathrm{s} = 980$ ($r = 248\,\mathrm{nm}$). As such to check the validity of the integral parameterisation, the limit was set at $\int_0^{248\,\mathrm{nm}} f(r)\,\mathrm{d}r$. For all wavelengths and fractal dimensions, agreement between the two methods is within 3 % for g and σ_sca, and within 0.15 % for σ_ext. Errors are slightly smaller than for individual scattering particles, since the parameterisation of individual particles roughly underestimates values as often as it overestimates.

The parameterisation is available as an Supplement to this work, and includes routines in the Interactive Data Language (IDL) to implement extinction, scattering, SSA, and asymmetry parameter calculations for individual particles and log-normal distributions.

4 Conclusions

It has been shown that it is not possible to model the optical properties of black carbon fractal aggregates using spheres with refractive indices in the range $0 \le m_\mathrm{BC} \le 3+3i$ at any wavelength between 400 nm and 15 µm. Other approximations such as RDG can improve greatly the representation of BCFA optical properties but generally do not provide sufficient absorption. With this in mind, a prudent step for GCMs requiring constantly changing distributions of BC aerosol could be to include a parameterisation such as this one which is computationally trivial to implement and is valid within the range of black carbon particles seen in the atmosphere. Uncertainties in the size distribution, shape, and composition of these particles should not be

forgotten and will certainly cause differences at least as large as the simplification of optical properties to spheres or RDG.

Acknowledgement. The authors acknowledge funding from the UK Natural Environment Research Council (NERC) National Centre for Earth Observation and the NERC project NE/F018142/1.

References

Abel, S. J., Haywood, J. M., Highwood, E. J., Li, J., and Buseck, P. R.: Evolution of biomass burning aerosol properties from an agricultural fire in southern Africa, Geophys. Res. Lett., 30, 1783, doi:10.1029/2003GL017342, 2003.

Adachi, K., Chung, S. H., and Buseck, P. R.: Shapes of soot aerosol particles and implications for their effects on climate, J. Geophys. Res., 115, D15206, doi:10.1029/2009JD012868, 2010.

Bahadur, R., Feng, Y., Russell, L. M., and Ramanathan, V.: Impact of California's air pollution laws on black carbon and their implications for direct radiative forcing, Atmos. Environ., 45, 1162–1167, doi:10.1016/j.atmosenv.2010.10.054, 2011.

Bambha, R. P., Dansson, M. A., Schrader, P. E., and Michelsen, H. A.: Effects of volatile coatings on the laser-induced incandescence of soot, Appl. Phys. B, 112, 343–358, doi:10.1007/s00340-013-5463-9, 2013.

Bohren, C. F. and Huffman, D. R.: Absorption and Scattering of Light by Small Particles, Wiley-VCH, doi:10.1002/9783527618156, 1983.

Bond, T. C.: Can warming particles enter global climate discussions?, Environ. Res. Lett., 2, 045030, doi:10.1088/1748-9326/2/4/045030, 2007.

Bond, T. C. and Bergstrom, R. W.: Light absorption by carbonaceous particles: an investigative review, Aerosol Sci. Tech., 40, 27–67, doi:10.1080/02786820500421521, 2006.

Bond, T. C., Streets, D. G., Yarber, K. F., Nelson, S. M., Woo, J.-H., and Klimont, Z.: A technology-based global inventory of black and organic carbon emissions from combustion, J. Geophys. Res., 109, D14203, doi:10.1029/2003JD003697, 2004.

Bond, T. C., Habib, G., and Bergstrom, R. W.: Limitations in the enhancement of visible light absorption due to mixing state, J. Geophys. Res., 111, D20211, doi:10.1029/2006JD007315, 2006.

Bond, T. C., Doherty, S. J., Fahey, D. W., Forster, P. M., Berntsen, T., DeAngelo, B. J., Flanner, M. G., Ghan, S., Kärcher, B., Koch, D., Kinne, S., Kondo, Y., Quinn, P. K., Sarofim, M. C., Schultz, M. G., Schulz, M., Venkataraman, C., Zhang, H., Zhang, S., Bellouin, N., Guttikunda, S. K., Hopke, P. K.,

Jacobson, M. Z., Kaiser, J. W., Klimont, Z., Lohmann, U., Schwarz, J. P., Shindell, D., Storelvmo, T., Warren, S. G., and Zender, C. S.: Bounding the role of black carbon in the climate system: a scientific assessment, J. Geophys. Res., 118, 5380–5552, doi:10.1002/jgrd.50171, 2013.

Buseck, P. R., Huang, B., and Keller, L. P.: Electron microscope investigation of the structures of annealed carbons, Energ. Fuel., 1, 105–110, doi:10.1021/ef00001a020, 1987.

Calcote, H. F.: Mechanisms of soot nucleation in flames – a critical review, Combust. Flame, 42, 215–242, doi:10.1016/0010-2180(81)90159-0, 1981.

Cappa, C. D., Onasch, T. B., Massoli, P., Worsnop, D. R., Bates, T. S., Cross, E. S., Davidovits, P., Hakala, J., Hayden, K. L., Jobson, B. T., Kolesar, K. R., Lack, D. A., Lerner, B. M., Li, S.-M., Mellon, D., Nuaaman, I., Olfert, J. S., Petäjä, T., Quinn, P. K., Song, C., Subramanian, R., Williams, E. J., and Zaveri, R. A.: Radiative Absorption Enhancements Due to the Mixing State of Atmospheric Black Carbon, Science, 337, 1078–1081, doi:10.1126/science.1223447, 2012.

Cappa, C. D., Onasch, T. B., Massoli, P., Worsnop, D. R., Bates, T. S., Cross, E. S., Davidovits, P., Hakala, J., Hayden, K. L., Jobson, B. T., Kolesar, K. R., Lack, D. A., Lerner, B. M., Li, S.-M., Mellon, D., Nuaaman, I., Olfert, J. S., Petäjä, T., Quinn, P. K., Song, C., Subramanian, R., Williams, E. J., and Zaveri, R. A.: Response to Comment on "Radiative Absorption Enhancements Due to the Mixing State of Atmospheric Black Carbon", Science, 339, 393, doi:10.1126/science.1230260, 2013.

Chang, H. and Charalampopoulos, T. T.: Determination of the wavelength dependence of refractive indices of flame soot, P. Roy. Soc. Lond. A Mat., 430, 577–591, doi:10.1098/rspa.1990.0107, 1990.

Dockery, D. W., Pope, C. A., Xu, X., Spengler, J. D., Ware, J. H., Fay, M. E., Ferris, B. G., and Speizer, F. E.: An association between air pollution and mortality in six U. S. cities, New Engl. J. Med., 329, 1753–1759, doi:10.1056/NEJM199312093292401, 1993.

Doherty, S. J., Warren, S. G., Grenfell, T. C., Clarke, A. D., and Brandt, R. E.: Light-absorbing impurities in Arctic snow, Atmos. Chem. Phys., 10, 11647–11680, doi:10.5194/acp-10-11647-2010, 2010.

Flanner, M. G., Zender, C. S., Hess, P. G., Mahowald, N. M., Painter, T. H., Ramanathan, V., and Rasch, P. J.: Springtime warming and reduced snow cover from carbonaceous particles, Atmos. Chem. Phys., 9, 2481–2497, doi:10.5194/acp-9-2481-2009, 2009.

Fuller, K. A., Malm, W. C., and Kreidenweis, S. M.: Effects of mixing on extinction by carbonaceous particles, J. Geophys. Res., 104, 15941–15954, doi:10.1029/1998JD100069, 1999.

Grainger, R. G., Lucas, J., Thomas, G. E., and Ewen, G. B.: Calculation of Mie derivatives, Appl. Optics, 43, 5386–5393, doi:10.1364/AO.43.005386, 2004.

Gwaze, P., Schmid, O., Annegarn, H. J., Andreae, M. O., Huth, J. and Helas, G.: Comparison of three methods of fractal analysis applied to soot aggregates from wood combustion, J. Aerosol Sci., 37, 820–838, doi:10.1016/j.jaerosci.2005.06.007, 2006.

Helble, J., Neville, M., and Sarofim, A. F.: Aggregate formation from vaporized ash during pulverized coal combustion, Symposium (International) on Combustion, 21, 411–417, doi:10.1016/S0082-0784(88)80268-6, 1988.

Homann, K. H.: Carbon formation in premixed flames, Combust. Flame, 11, 265–287, doi:10.1016/0010-2180(67)90017-X, 1967.

Ito, A. and Penner, J. E.: Historical emissions of carbonaceous aerosols from biomass and fossil fuel burning for the period 1870–2000, Global Biogeochem. Cy., 19, GB2028, doi:10.1029/2004GB002374, 2005.

Jacobson, M. Z.: Strong radiative heating due to the mixing state of black carbon in atmospheric aerosols, Nature, 409, 695–697, doi:10.1038/35055518, 2001.

Jacobson, M. Z.: Control of fossil-fuel particulate black carbon and organic matter, possibly the most effective method of slowing global warming, J. Geophys. Res., 107, 4410, doi:10.1029/2001JD001376, 2002.

Jacobson, M. Z.: Reply to comment by J. E. Penner on "Control of fossil-fuel particulate black carbon and organic matter, possibly the most effective method of slowing global warming", J. Geophys. Res., 108, 4772, doi:10.1029/2003JD003403, 2003.

Jacobson, M. Z.: Comment on "Radiative Absorption Enhancements Due to the Mixing State of Atmospheric Black Carbon", Science, 339, 393, doi:10.1126/science.1229920, 2013.

Jansen, K. L., Larson, T. V., Koenig, J. Q., Mar, T. F., Fields, C., Stewart, J., and Lippmann, M.: Associations between health effects and particulate matter and black carbon in subjects with respiratory disease, Environ. Health Persp., 113, 1741–1746, doi:10.1289/ehp.8153, 2005.

Kahnert, M.: On the Discrepancy between Modeled and Measured Mass Absorption Cross Sections of Light Absorbing Carbon Aerosols, Aerosol Sci. Tech., 44, 453–460, doi:10.1080/02786821003733834, 2010a.

Kahnert, M.: Numerically exact computation of the optical properties of light absorbing carbon aggregates for wavelength of 200 nm–12.2 µm. Atmos. Chem. Phys., 10, 8319-–8329, 44, 453–460, doi:10.5194/acp-10-8319-2010, 2010b.

Larson, S. M., Cass, G. R., and Gray, H. A.: Atmospheric carbon particles and the Los Angeles visibility problem, Aerosol Sci. Tech., 10, 118–130, doi:10.1080/02786828908959227, 1989.

Li, H., Liu, C., Bi, L., Yang, P., and Kattawar, G. W.: Numerical accuracy of "equivalent" spherical approximations for computing ensemble-averaged scattering properties of fractal soot aggregates, J. Quant. Spectrosc. Ra., 111, 2127–2132, doi:10.1016/j.jqsrt.2010.05.009, 2010.

Li, J., Pósfai, M., Hobbs, P. V., and Buseck, P. R.: Individual aerosol particles from biomass burning in southern Africa: 2. Compositions and aging of inorganic particles, J. Geophys. Res., 108, 8484, doi:10.1029/2002JD002310, 2003.

Liu, L. and Mishchenko, M. I.: Effects of aggregation on scattering and radiative properties of soot aerosols, J. Geophys. Res., 110, D11211, doi:10.1029/2004JD005649, 2005.

Liu, L., Mishchenko, M. I., and Arnott, W. P.: A study of radiative properties of fractal soot aggregates using the superposition T-matrix method, J. Quant. Spectrosc. Ra., 109, 2656–2663, doi:10.1016/j.jqsrt.2008.05.001, 2008.

Liu, C., Panetta, R. L., and Yang, P.: The Influence of Water Coating on the Optical Scattering Properties of Fractal Soot Aggregates, Aerosol Sci. Tech., 46, 31–43, doi:10.1080/02786826.2011.605401, 2012.

Mackowski, D. W.: MSTM – a multiple sphere T-matrix FORTRAN code for use on parallel computer clusters, Department of Mechanical Engineering, Auburn University, Auburn, AL 36849, USA, available at: http://eng.auburn.edu/users/dmckwski/scatcodes (last access: June 2013), 2012.

Mackowski, D. W. and Mishchenko, M. I.: Calculation of the T-matrix and the scattering matrix for ensembles of spheres, J. Opt. Soc. Am. A., 13, 2266–2278, doi:10.1364/JOSAA.13.002266, 1996.

Martins, J. V., Artaxo, P., Liousse, C., Reid, J. S., Hobbs, P. V., and Kaufman, Y. J.: Effects of black carbon content, particle size, and mixing on light absorption by aerosols from biomass burning in Brazil, J. Geophys. Res., 103, 32041–32050, doi:10.1029/98JD02593, 1998a.

Martins, J. V., Hobbs, P. V., Weiss, R. E., and Artaxo, P.: Sphericity and morphology of smoke particles from biomass burning in Brazil, J. Geophys. Res., 103, 32051–32057, doi:10.1029/98JD01153, 1998b.

Mie, G.: Beiträge zur Optik trüber Medien, speziell kolloidaler Metallösungen, Ann. Phys., 25, 377–445, a translation can be found at http://diogenes.iwt.uni-bremen.de/vt/laser/papers/RAE-LT1873-1976-Mie-1908-translation.pdf (last access: 15 March 2011), 1908.

Mikhailov, E. F., Vlasenko, S. S., Podgorny, I. A., Ramanathan, V., and Corrigan, C. E.: Optical properties of soot–water drop agglomerates: An experimental study, J. Geophys. Res., 111, D07209, doi:10.1029/2005JD006389, 2006.

Popovicheva, O., Persiantseva, N. M., Shonija, N. K., DeMott, P., Koehler, K., Petters, M., Kreidenweis, S., Tishkova, V., Demirdjian, B., and Suzanne, J.: Water interaction with hydrophobic and hydrophilic soot particles, Phys. Chem. Chem. Phys., 10, 2332–2344, doi:10.1039/b718944n, 2008.

Pósfai, M., Anderson, J. R., Buseck, P. R., and Sievering, H.: Soot and sulfate aerosol particles in the remote marine troposphere, J. Geophys. Res., 104, 21685–21693, doi:10.1029/1999JD900208, 1999.

Reid, J. S., Koppmann, R., Eck, T. F., and Eleuterio, D. P.: A review of biomass burning emissions part II: intensive physical properties of biomass burning particles, Atmos. Chem. Phys., 5, 799–825, doi:10.5194/acp-5-799-2005, 2005.

Rodgers, C. D.: Inverse Methods for Atmospheric Sounding: Theory and Practice, vol. 2 of Atmospheric, Oceanic and Planetary Physics, World Scientific Publishing Co., 2000.

Scarnato, B. V., Vahidinia, S., Richard, D. T., and Kirchstetter, T. W.: Effects of internal mixing and aggregate morphology on optical properties of black carbon using a discrete dipole approximation model, Atmos. Chem. Phys., 13, 5089, doi:10.5194/acp-13-5089-2013, 2013.

Sorensen, C. M.: Light scattering by fractal aggregates: a review, Aerosol Sci. Tech., 35, 648–687, doi:10.1080/02786820117868, 2001.

Stier, P., Seinfeld, J. H., Kinne, S., and Boucher, O.: Aerosol absorption and radiative forcing, Atmos. Chem. Phys., 7, 5237–5261, doi:10.5194/acp-7-5237-2007, 2007.

Streets, D. G., Bond, T. C., Carmichael, G. R., Fernandes, S. D., Fu, Q., He, D., Klimont, Z., Nelson, S. M., Tsai, N. Y., Wang, M. Q., Woo, J.-H., and Yarber, K. F.: An inventory of gaseous and primary aerosol emissions in Asia in the year 2000, J. Geophys. Res., 108, 8809, doi:10.1029/2002JD003093, 2003.

Su, D. S., Müller, J.-O., Jentoft, R. E., Rothe, D., Jacob, E. and Schlögl, R.: Fullerene-like soot from EuroIV diesel engine: consequences for catalytic automotive pollution control, Top. Catal., 30–31, 241–245, doi:10.1023/B:TOCA.0000029756.50941.02, 2004.

Thouy, R. and Jullien, R.: A cluster–cluster aggregation model with tunable fractal dimension, J. Phys. A-Math. Gen., 27, 2953, doi:10.1088/0305-4470/27/9/012, 1994.

Turns, S. R.: An Introduction to Combustion – Concepts and Applications, 2nd edn., McGraw-Hill, 2000.

Yin, J. Y. and Liu, L. H.: Influence of complex component and particle polydispersity on radiative properties of soot aggregate in atmosphere, J. Quant. Spectrosc. Ra., 111, 2115–2126, doi:10.1016/j.jqsrt.2010.05.016, 2010.

Zhang, R., Khalizov, A. F., Pagels, J., Zhang, D., Xue, H., and McMurry, P. H.: Variability in morphology, hygroscopicity, and optical properties of soot aerosols during atmospheric processing, P. Natl Acad. Sci. USA, 105, 10291–10296, doi:10.1073/pnas.0804860105, 2008.

Zhao, Y. and Ma, L.: Applicable range of the Rayleigh–Debye–Gans theory for calculating the scattering matrix of soot aggregates, Appl. Optics, 48, 591–597, doi:10.1364/AO.48.000591, 2009.

Table 1. Fit coefficients for estimation of BCFA optical properties at $\lambda = 550\,\mathrm{nm}$ and $D_\mathrm{f} = 1.8$. Relative RMS errors for all fitted points, equally weighted are also given. The marked, lower values, "Rel.*" ignore the first two data points where $n_\mathrm{s} \leq 40$, showing that this is where the majority of the relative error is contained. While the values of coefficient 1 (the linear term) in the fits of SSA and g are negligible at 550 nm, they increase at longer wavelengths while the values of coefficient 2 (the logarithmic term) decrease.

Coeff.	σ_ext	SSA	g
0	-2.026×10^{3}	8.902×10^{-2}	2.669×10^{-1}
1	9.581×10^{2}	0.000×10^{0}	0.000×10^{0}
2	1.120×10^{-3}	2.876×10^{-2}	6.981×10^{-2}
3	4.110×10^{-6}	–	–
RMS error			
Rel.	0.50 %	2.53 %	5.02 %
Rel.*	0.25 %	1.64 %	2.13 %

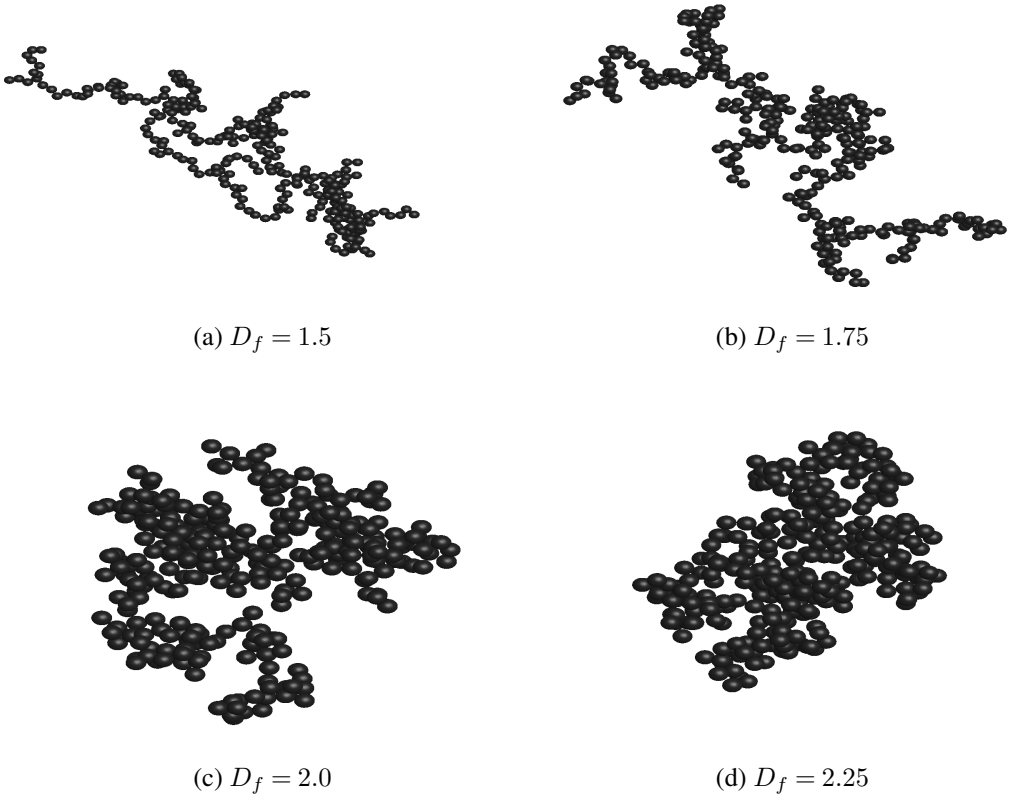

(a) $D_f = 1.5$ (b) $D_f = 1.75$

(c) $D_f = 2.0$ (d) $D_f = 2.25$

Fig. 1. Modelled fractal aggregates with n_s= 300, $k_\mathrm{f} = 1.25$ and varying values of D_f. As the fractal dimension increases, we move from linear to bunched clusters. These aggregates were generated using a cluster–cluster algorithm.

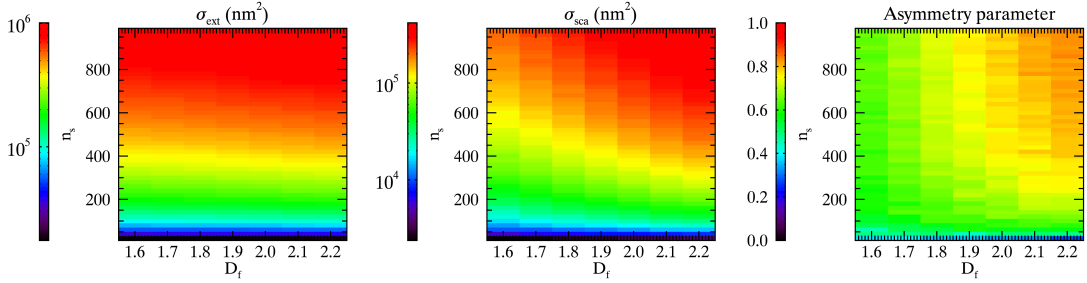

Fig. 2. Extinction cross-section, scattering cross-section, and asymmetry parameter calculated using the MSTM code at $\lambda = 550\,\mathrm{nm}$ for a range of fractal dimensions and numbers of spherules.

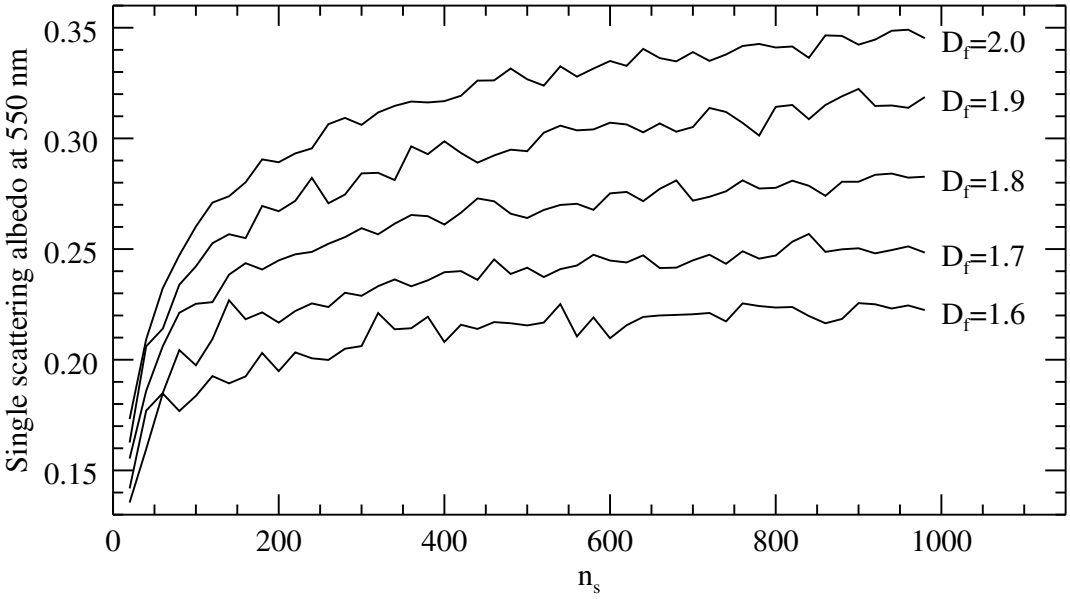

Fig. 3. The SSA of BCFAs at $\lambda = 550\,\mathrm{nm}$ as a function of n_s and D_f. The most likely values of D_f would be from 1.7–1.8, where the SSA values are between 0.2–0.3.

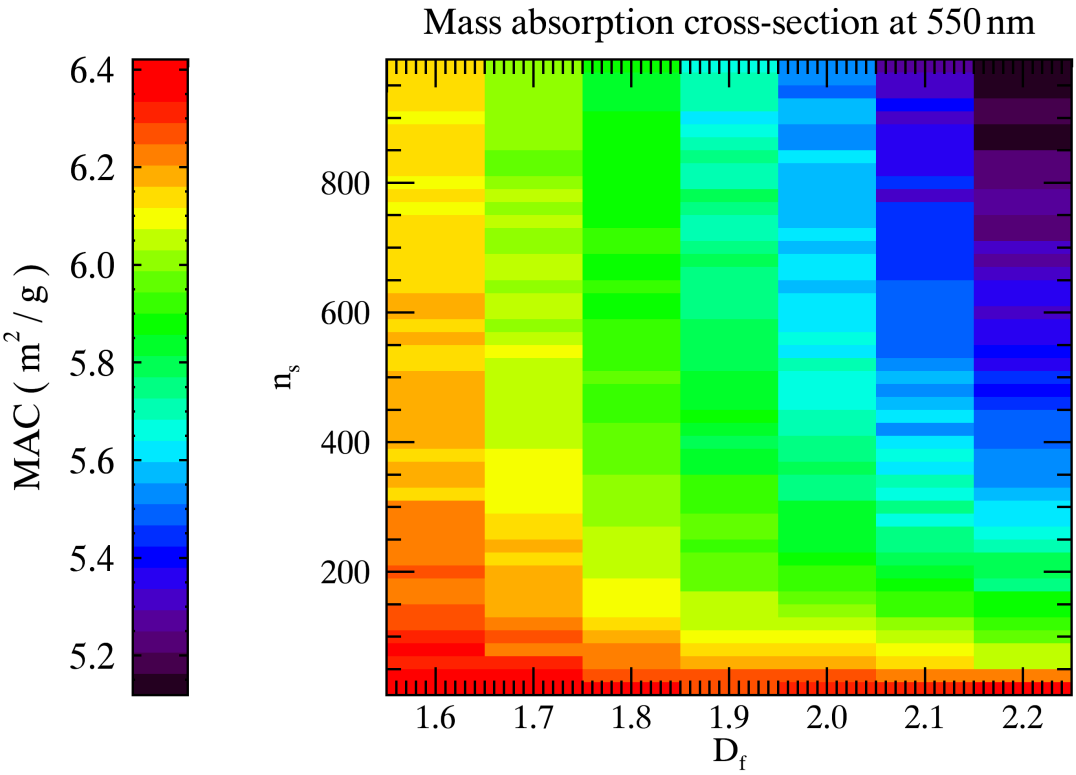

Fig. 4. The mass absorption cross section at $\lambda = 550\,\mathrm{nm}$ for BCFAs. This is the absorption cross section, divided by the mass of the particles. For these calculations, a density of $1.8\,\mathrm{g\,m^{-2}}$ was assumed.

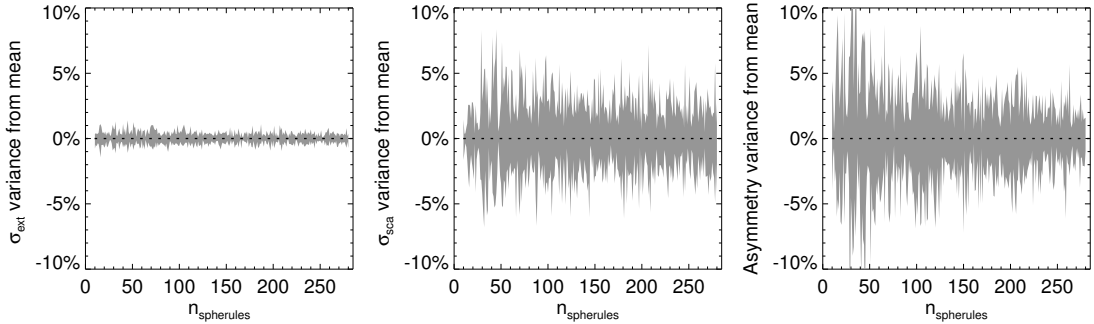

Fig. 5. Showing the envelope of relative spread from the mean of the three output parameters, σ_{ext}, σ_{sca} and g at $\lambda = 550\,\mathrm{nm}$, for BC with $D_{\mathrm{f}} = 1.75$, given four fractal geometries at each size. The high relative differences g with low n_{s} can be accounted for by the lower values of g in this regime.

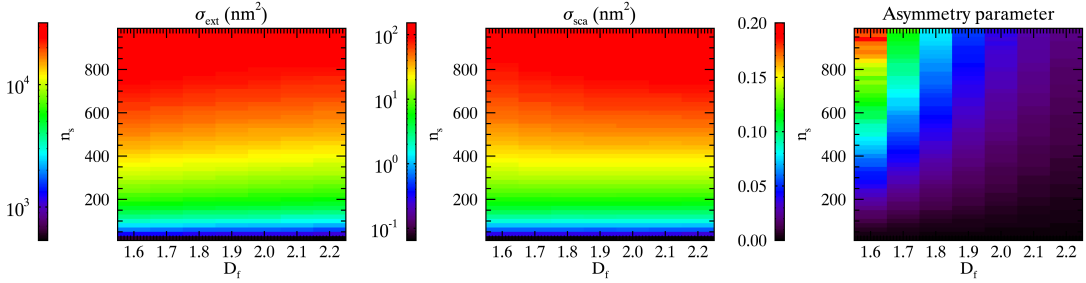

Fig. 6. Extinction cross-section, scattering cross-section, and asymmetry parameter calculated using the MSTM code at $\lambda = 12\,\mu\mathrm{m}$ for a range of fractal dimensions and numbers of spherules.

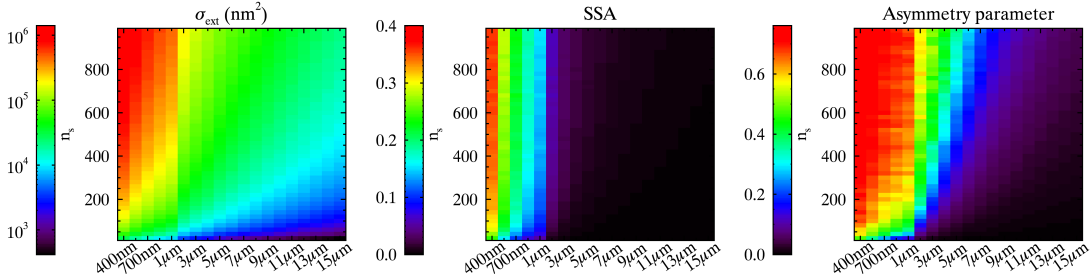

Fig. 7. Extinction cross-section, single scatter albedo, and asymmetry parameter calculated using the MSTM code at $D_{\mathrm{f}} = 1.8$. Note the discontinuity in wavelength step size at $\lambda = 1\,\mu\mathrm{m}$. Unlabeled wavelengths are half-way between the two values on either side.

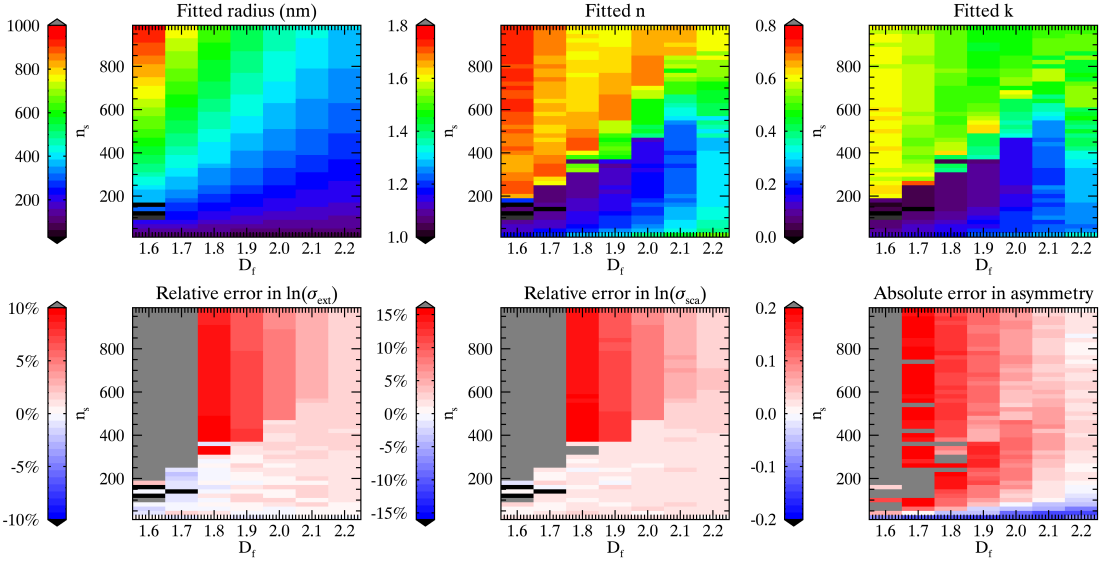

Fig. 8. The optimum fitted sphere parameters (r, n, and k) and their resultant errors relative to the reference MSTM calculations in $\ln\sigma_{\text{ext}}$, $\ln\sigma_{\text{sca}}$ and absolute errors in g for BCFAs with $\lambda = 550\,\text{nm}$. The colour scale has been adjusted so that the very large errors caused by unphysically small BCFA D_f are clipped.

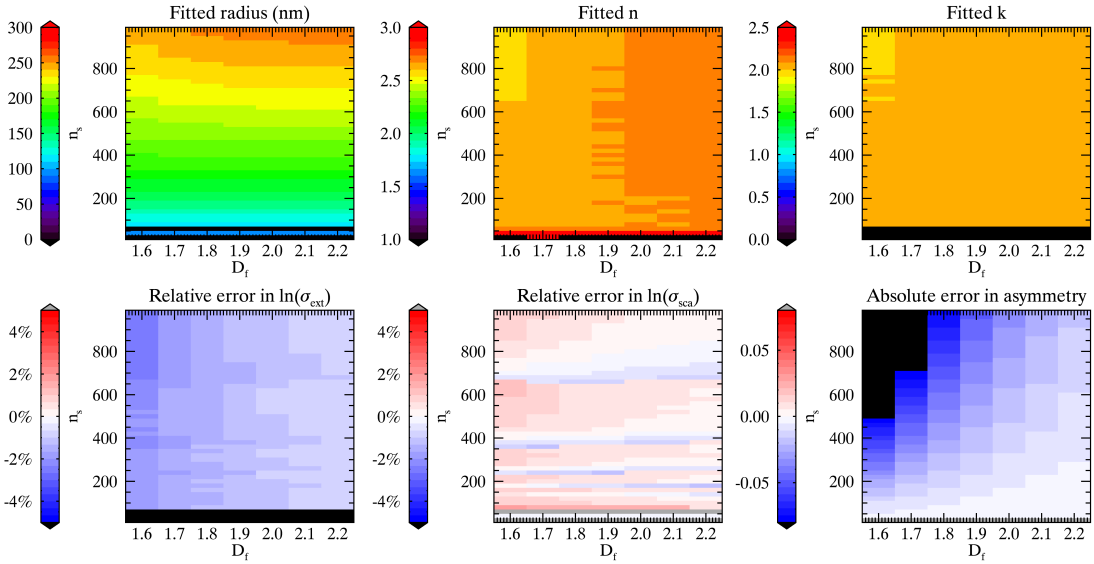

Fig. 9. The optimum fitted sphere parameters (r, n, and k) and their resultant relative errors in $\ln\sigma_{\mathrm{ext}}$, $\ln\sigma_{\mathrm{sca}}$ and absolute errors in g for $\lambda = 12\,\mu\mathrm{m}$. In this case, the errors on g have been allowed to be large in order to get good fits in the cross-sections. As a result, the fitted radius is close to the radius of equal volume (not shown), and the refractive indices are close to those used by the MSTM calculations ($m = 2.93 + 2.16i$).

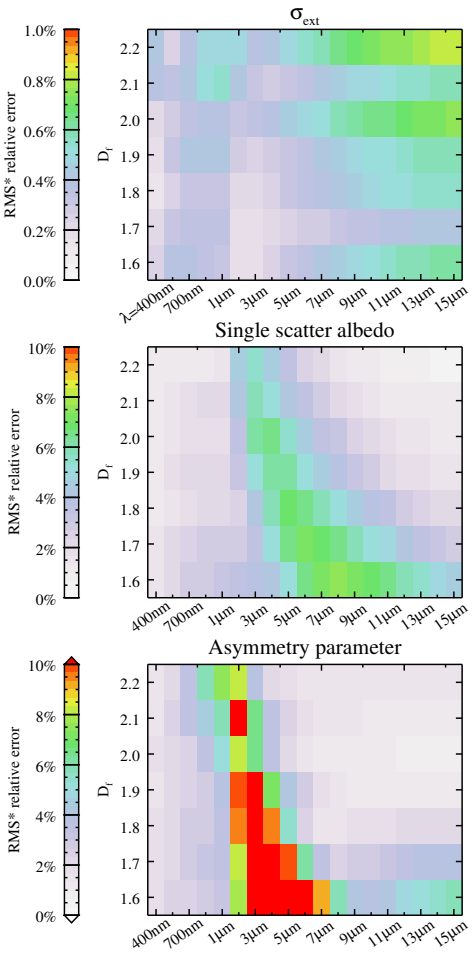

Fig. 10. The RMS relative errors between the calculated and parameterised values of σ_{ext}, SSA, and g. RMS calculations exclude the lowest two values of n_{s} as discussed in the text.

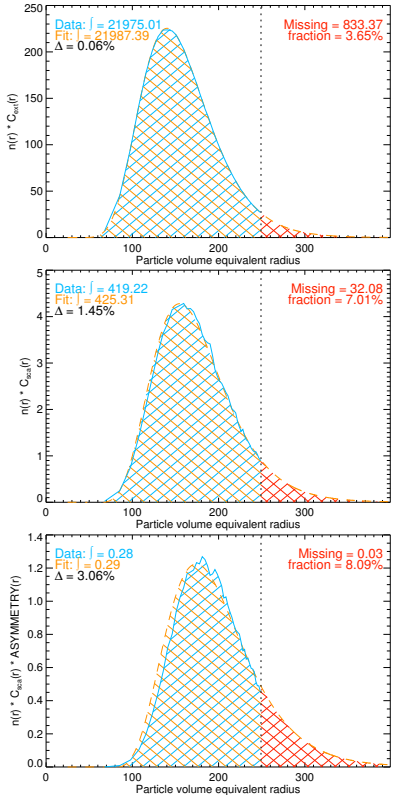

Fig. 11. Comparing the integrals of extinction, scattering, and asymmetry from a sum of fractal optical properties, and the parameterisations described in the text. Differences between the parameterised fit and the data are compared only for the area bounded by the maximum value of $n_s = 980$. These calculations are for $D_f = 1.8$ and $\lambda = 2\,\mu m$. The MSTM calculations (Data) are blue, the fitted data for the same radii (Fit) are orange, and the missing area covered by the fit, but not the MSTM calculations (Missing) are red. Numbers in these colours give the area under the respective curves. Δ gives the difference in areas between Data and Fit. The missing fraction is the fractional volume of Fit, not covered by Data.